

Mini-Workshop on Traps for Highly-exotic (highly-charged, highly-excited, rare isotope, anti-) States of Matter in POSTECH

## EBIT관련 원자 데이터, 분광 모델링 연구

### 현황 소개

권 덕 희

2025. 7. 11



Korea Atomic Energy  
Research Institute

Nuclear Physics Application Research Division

E-mail: [hkwon@kaeri.re.kr](mailto:hkwon@kaeri.re.kr)  
<https://pearl.kaeri.re.kr>



# Contents

- Atomic process in plasma
- EBIT for highly charged ions and the spectroscopic modeling
- Optical emission spectroscopy (OES) and collisional-radiative (CR) modeling for low temperature and low density plasma (Ar, He, H, atom and lowly charged ions)
- Summary and outlook

# Atomic processes in plasma



- Atoms and ions in plasma are neither isolated single atom/ion nor simple approach for two, three,... levels is applicable.
- Various collision processes with electrons and ions have to be considered for the spectral line intensity.

$$I_{ji} = \frac{1}{4\pi d^2} \int G_{ji}(T_e, n_e, \dots) dV$$
$$G_{ji}(T_e, n_e, \dots) = \frac{n_j(A^{q+})}{n(A^{q+})} \frac{n(A^{q+})}{n(A)} A_{ji}$$

Fractional abundance  
for charge state  
distribution

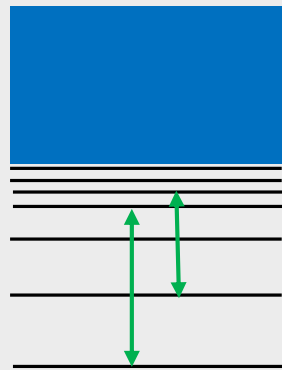
A diagram showing a fraction  $\frac{n(A^{q+})}{n(A)}$  enclosed in a light blue rounded rectangle. An arrow points from this fraction to the symbol  $A_{ji}$  in the equation below it.

- Accuracies of the collision process data are essential for the reliability of plasma spectroscopy.

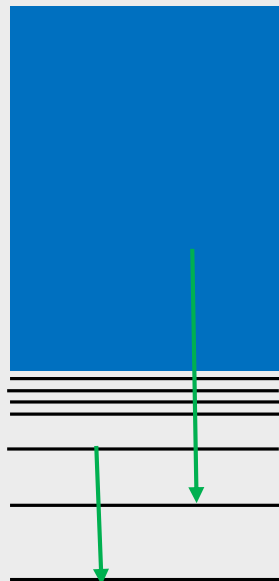
# Atomic processes in plasma



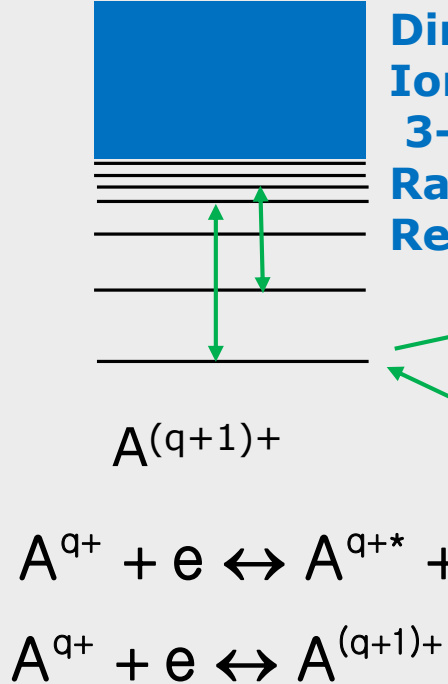
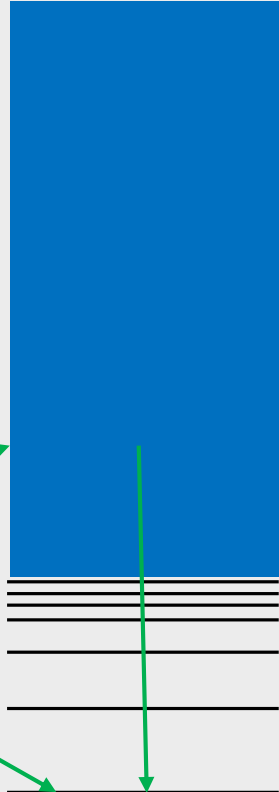
## Collisional (De)excitation



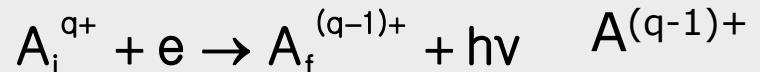
## Radiative Decays



## Autoionization/ Dielectronic Recombination (DR)

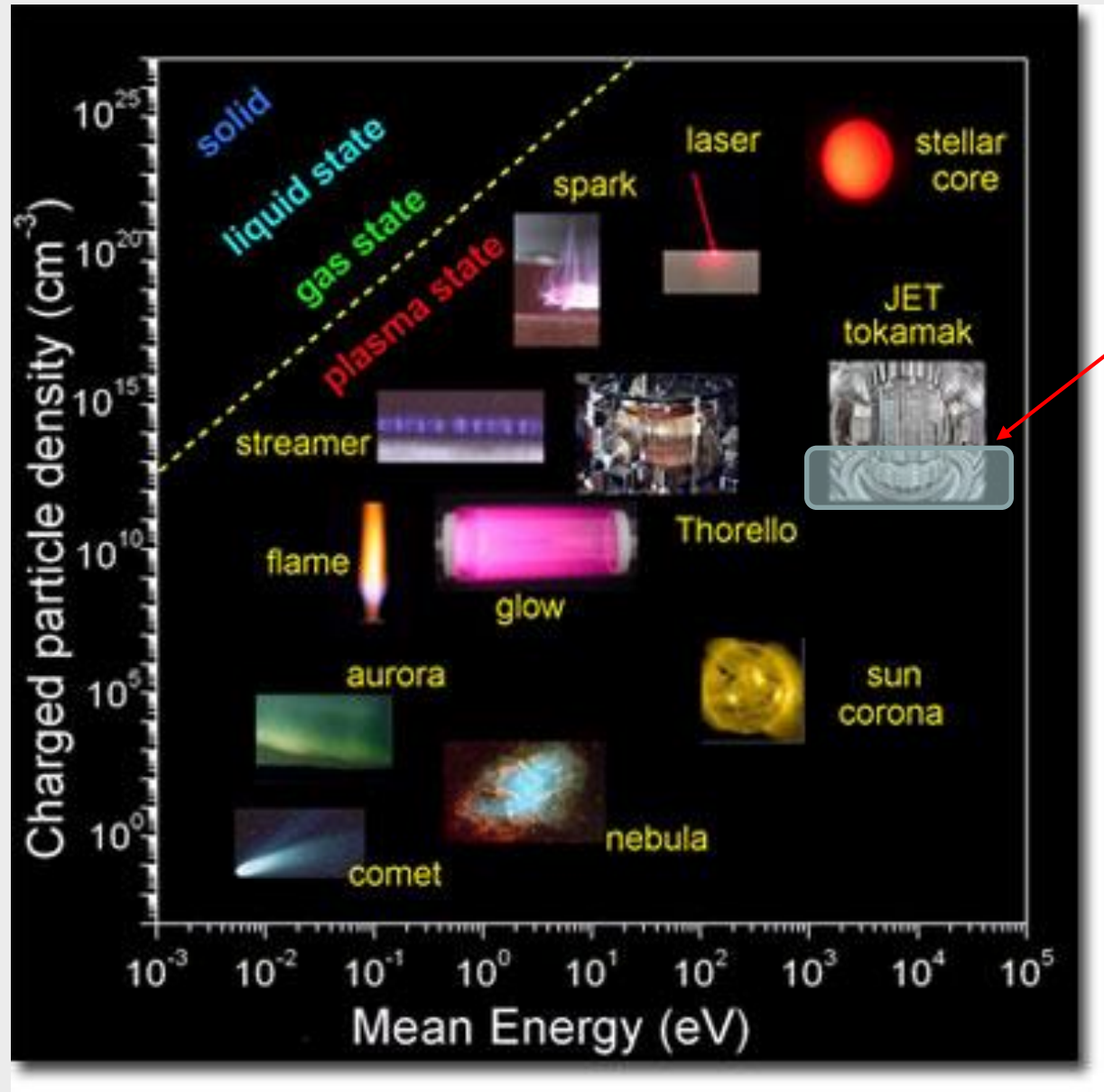


## Radiative Recombination (RR)



**Heavy particle collisions such as charge exchange, penning ionization etc.**

# Temperatures and densities for various plasmas



**EBIT**  
 $\sim 1\text{--}200 \text{ keV}$   
 $\sim 10^{13} \text{ cm}^{-3}$

**Tunable, Non-Maxwellian Quasi-monoenergetic**  
electron beams enabling to selective charge state and excitation  
  
Well-suited for studies of **electron impact excitation, ionization, radiative, dielectronic recombination, and identification of transitions from highly charged ions (HCIs)**

# EBIT as essential spectroscopic tools



- HCIs are abundant in the visible ***universe*** such as stars, galaxies and their clusters or the intergalactic medium as well as in ***laboratory plasmas*** including ***fusion plasmas***. EBITs are used to accurately measure the ***wavelengths of spectral lines*** emitted by HCIs to ***identify and diagnose*** the charge states and behavior of impurities in fusion plasmas.
- In atomic physics, fundamental interactions due to relativistic effects, quantum electrodynamics (***QED***), and nuclear-size contributions of HCI are enhanced by several orders of magnitude compared to neutral or singly charged systems. So the *precise determination* of the ***electron mass*** and the ***electron magnetic moment*** as well as stringent QED tests. Moreover, several proposals contemplate HCIs as ideal laboratory probes of a possible variation of the ***fine-structure constant*** and ***as frequency references for optical clocks*** superior to state-of-the-art optical lattice or singly charged ion clocks.
- Other applications are ***tumor ion therapy*** and ***EUV nanolithography*** ...
- EBIT provides HCI as the ***target for x-ray photons*** at ***synchrotron or FEL facilities***.

# Models for population kinetics in plasma

- Thermodynamic equilibrium (TE) : Ideal plasma and radiation field at constant  $T$  whose physical states are described as
  - ✓ Radiation field given by Plank's law
  - ✓ Particles by Maxwellian energy distribution
  - ✓ Level population densities by Boltzmann relation
  - ✓ Ion stage densities by Saha equation
  - ✓ Inverse process by detailed balance
- Local thermodynamic equilibrium (LTE) : High density plasma where collisions are so dominated that maintain steady state population densities by the Boltzmann and ionization stages by the Saha equation

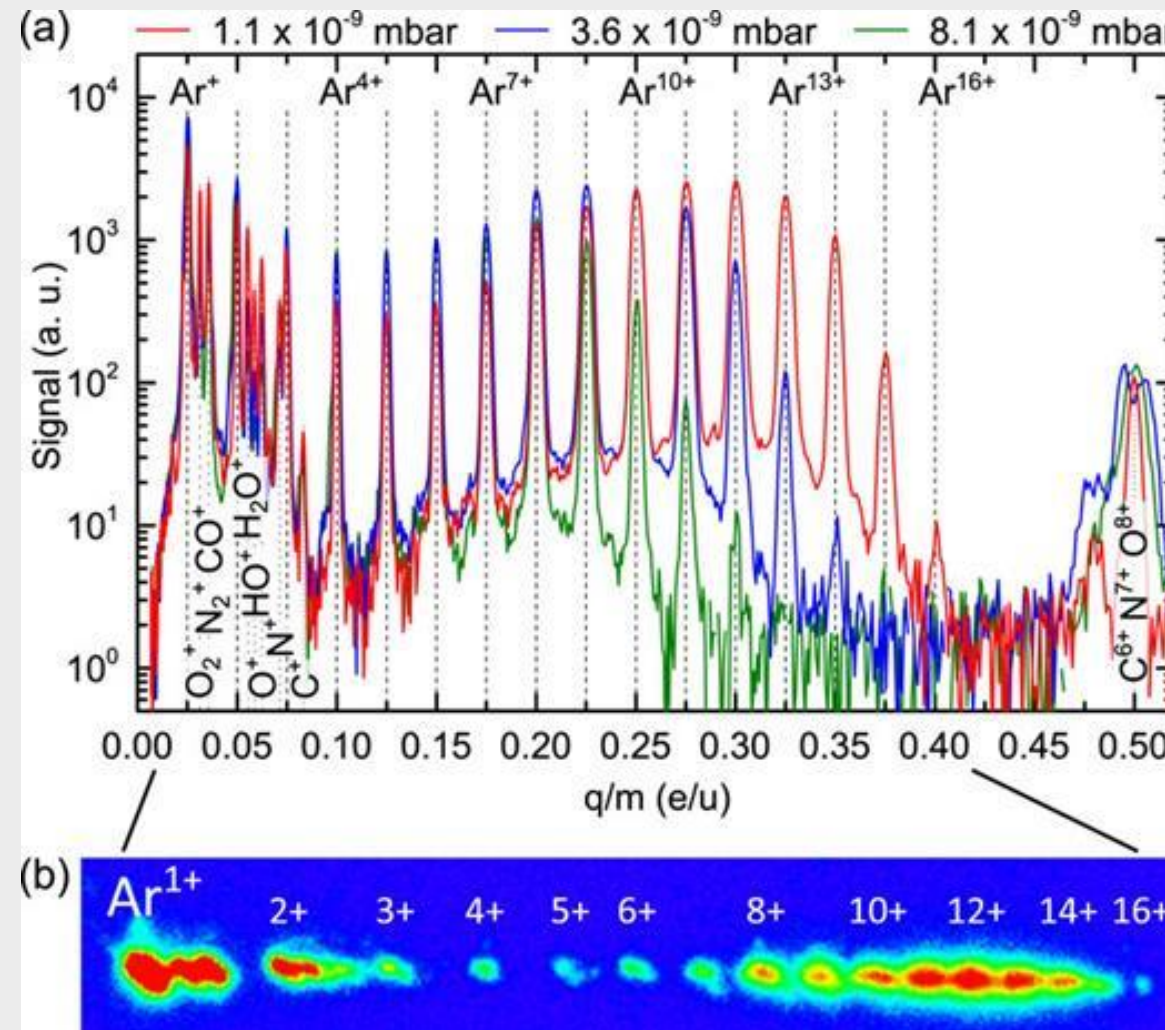
- **Collisional-radiative (CR)** : All possible collisional and radiative process are considered with external terms

$$\frac{dn_z(p)}{dt} = -R_z(p \rightarrow) + R_z(\rightarrow p) + \Gamma_z(p)$$

- Corona : low density plasma where

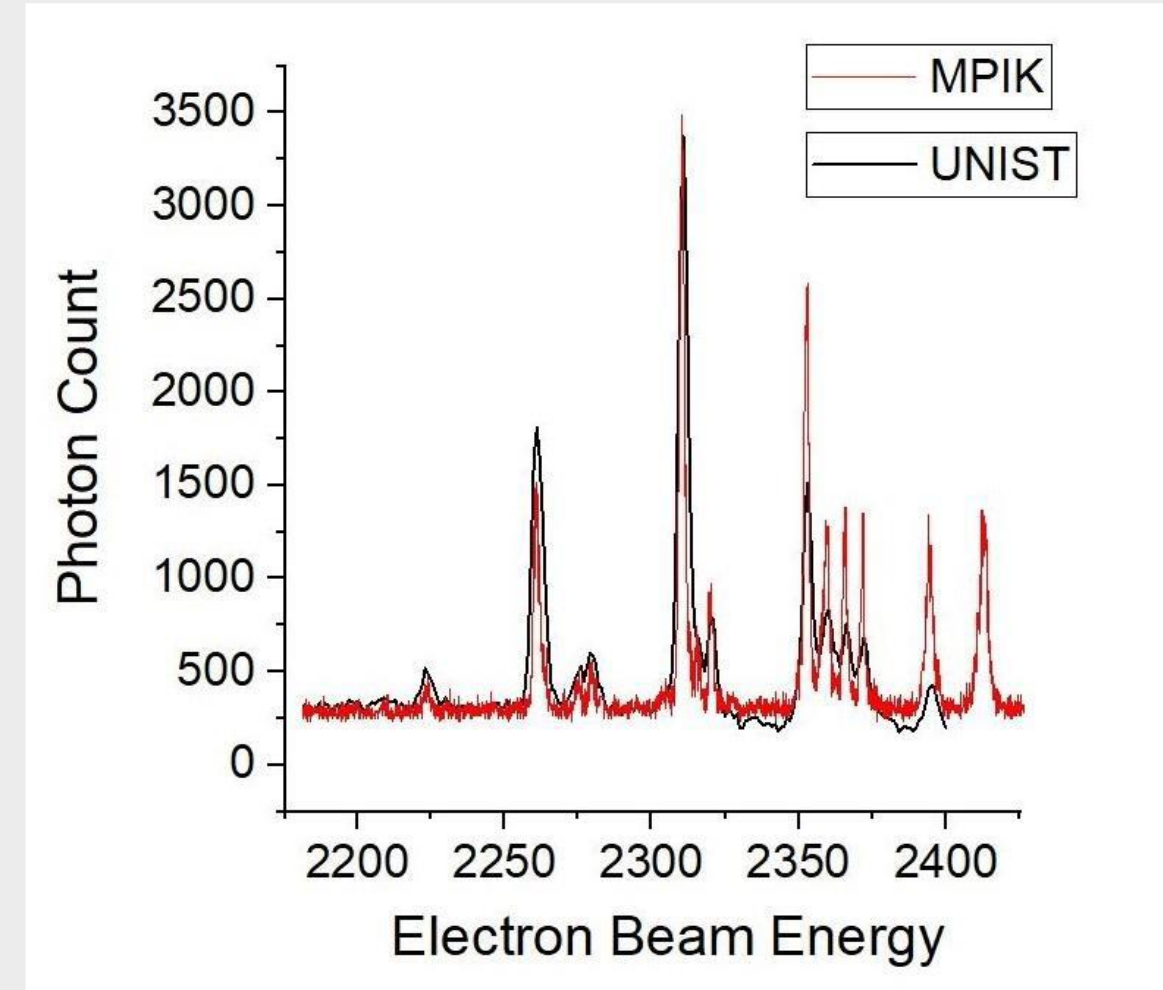
$$n_z(p)A_z(p \rightarrow) = n_e \sum_q n_z(q) X_z(q \rightarrow p), \quad n_e n_z S_z = n_e n_{z+1} \alpha_{z+1}$$

# Ar ( $Z=18$ , $1s^2$ $2s^2$ $2p^6$ $3s^2$ $3p^6$ ) ions from EBITs



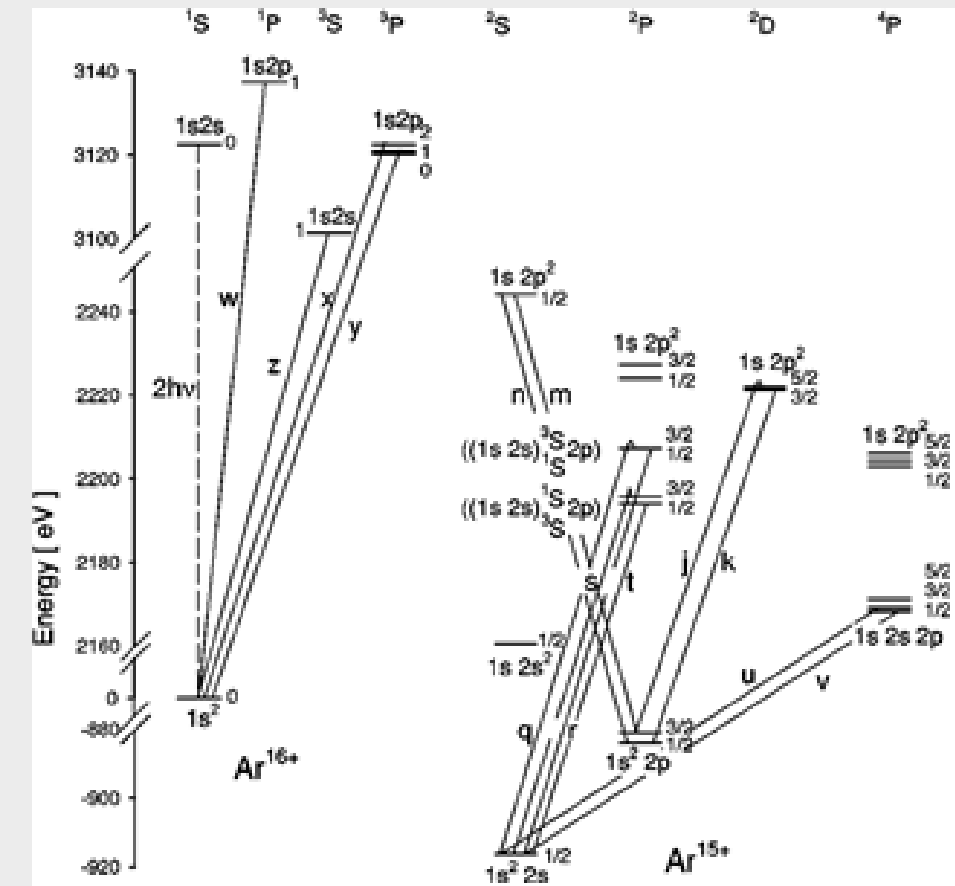
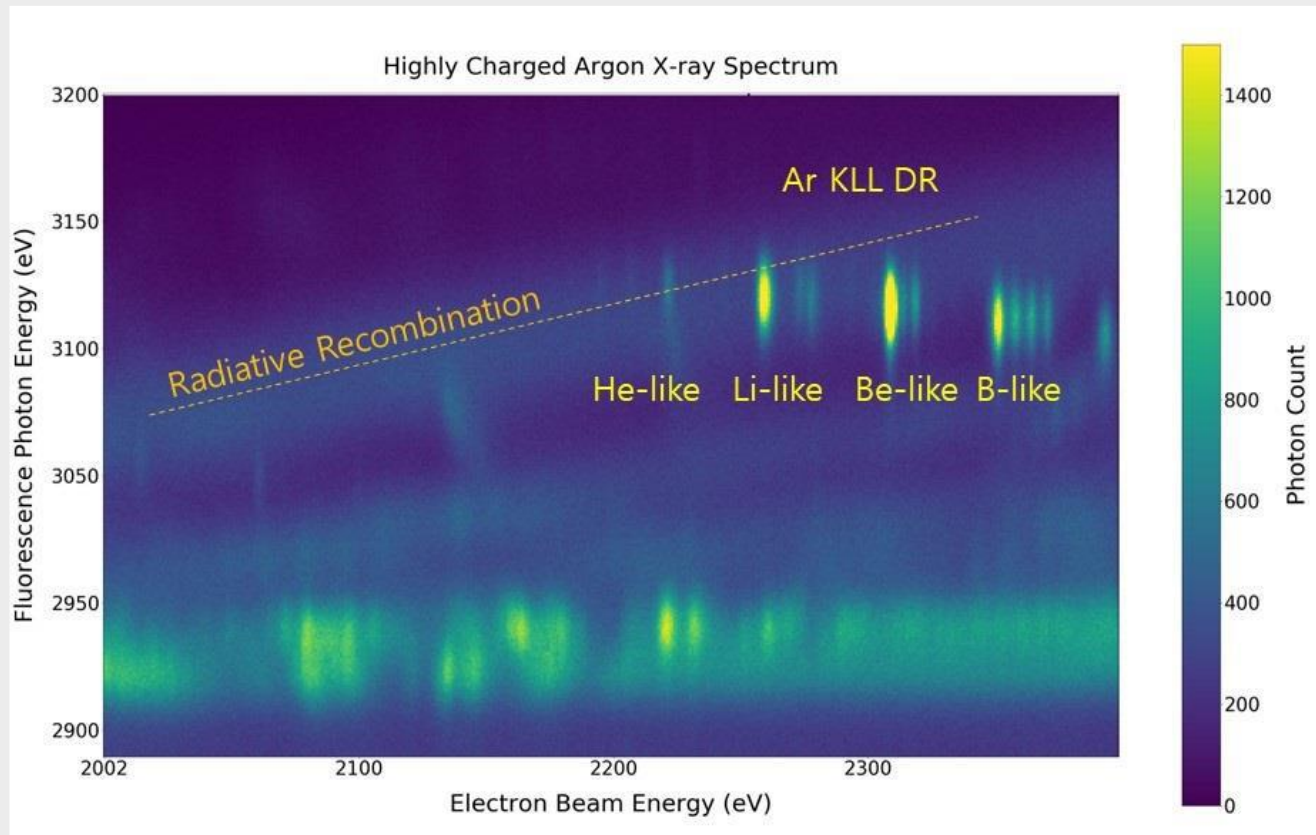
From: The Heidelberg compact electron beam ion traps

*Rev. Sci. Instrum.* 89, 063109 (2018)



## **On the courtesy of Dr. S. N. Park**

# RR and DR spectra from EBITs

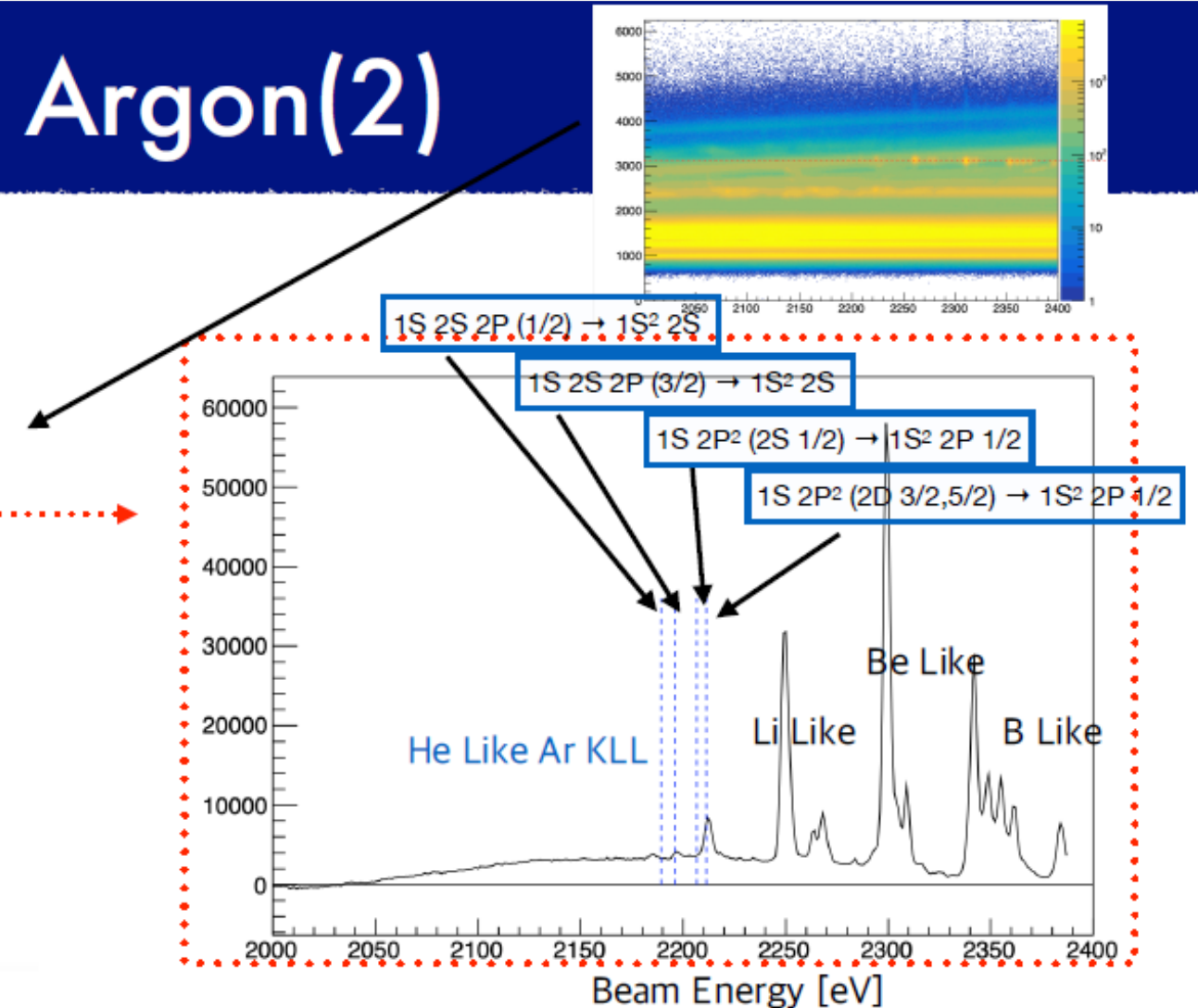
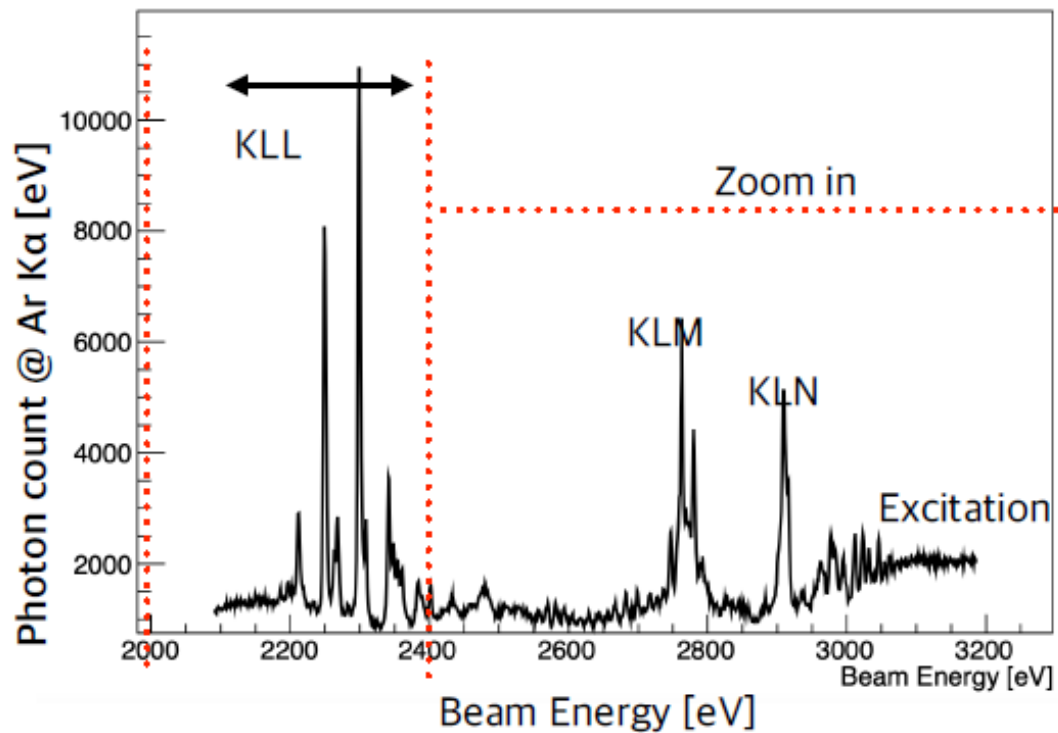


On the courtesy of Dr. S. N. Park

Energy levels and radiative transitions for He-like and Li-like Ar ions

# Benchmark Test Using Argon(2)

On the courtesy of Dr. B. Shin

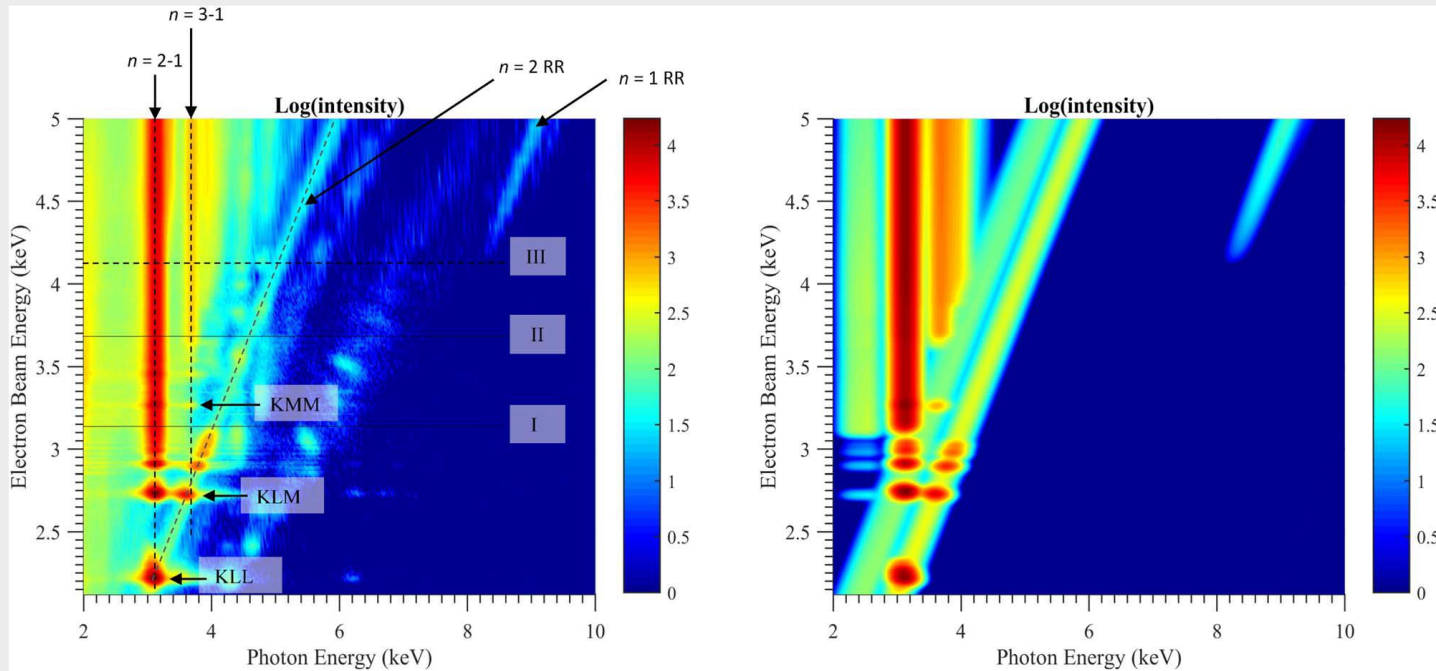


We confirmed "He Like Ar" ions were generated

To generate more He Like Ar, we will make more higher vacuum

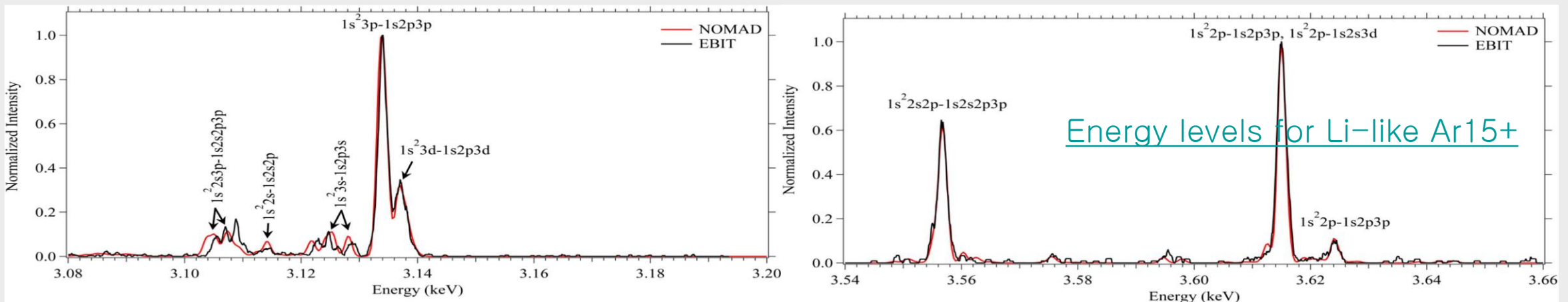
Target:  $6E-9$  mBar  $\Rightarrow$  less than  $1E-9$  mbar, Drift tube cleaning, Add up NEG pump

# CR modeling for EBIT



EBIT (NIST) and theoretical spectra at an electron beam energy of 2.730 keV

(A. C. Gall, ..., Y. Ralchenko, et al., *Astrophysical Journal*, **872**:194 2019)



# CR modeling for EBIT

**NOMAD (Non-Maxwellian, Arbitrary Distribution) CR code by Yuri Ralchenko**

$$\frac{d\hat{N}(t)}{dt} = \hat{A}(N_i, N_e, f_e, t)\hat{N}(t) + \hat{S}(t), \quad N_e(t) = N_e^0(t) + N_i(t) \sum_{Z=Z_{\min}}^{Z_{\max}} (Z-1) \sum_{k=1}^{k_{\max}} N_{Z,k}(t),$$

$$\hat{N}(t=0) = \hat{N}_0,$$

$$\sum_{Z=Z_{\min}}^{Z_{\max}} \sum_{k=1}^{k_{\max}} N_{Z,k}(t) = 1$$

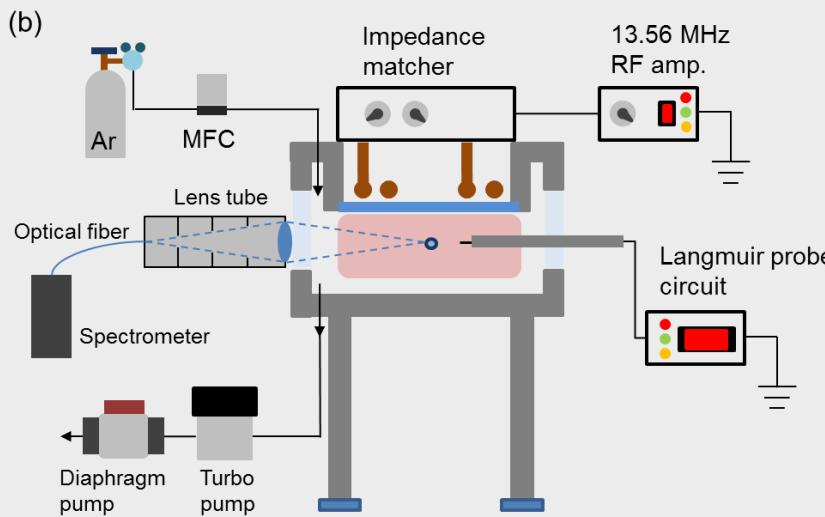
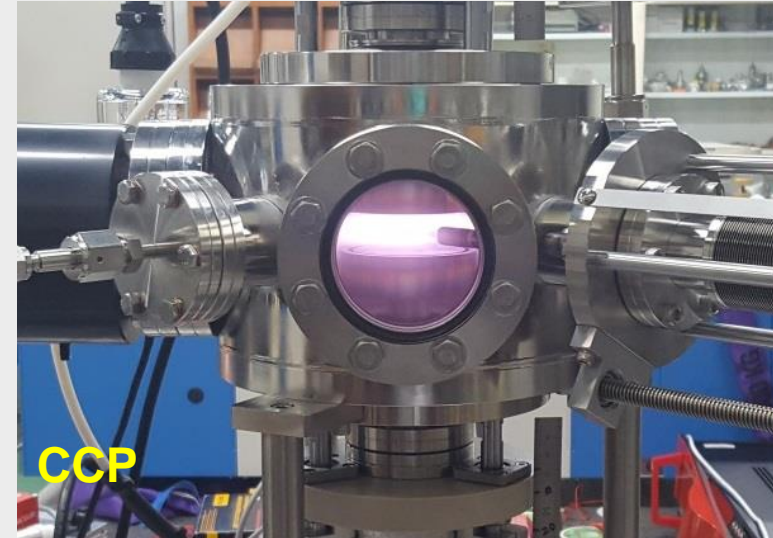
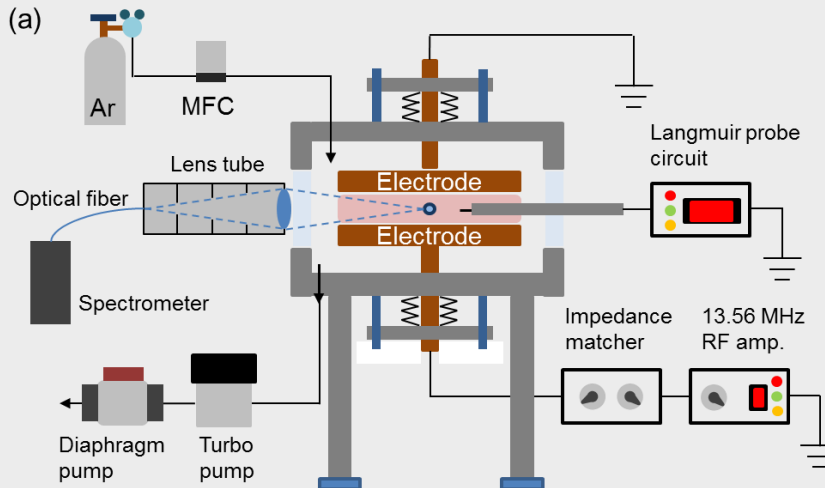
$$\sum_{j>i} N_{z,j} \cdot (A_{z,ij}^{rad} + n_e R_{z,ij}^{dx}) + \sum_{j< i} N_{z,j} n_e R_{z,ij}^{ex} + \sum_k n_e R_{z-1,ki}^{ion} + \sum_k n_e R_{z+1,ki}^{rr} + \delta_{i1} n_0 R_{z+1}^{cx}$$

$$-N_{z,i} \left( \sum_{j< i} (A_{z,ji}^{rad} + n_e R_{z,ji}^{dx}) + \sum_{j> i} n_e R_{z,ji}^{ex} + \sum_k n_e R_{z,ki}^{ion} + \sum_m n_e R_{z,mi}^{rr} + \delta_{i1} n_0 R_z^{cx} \right) = 0$$

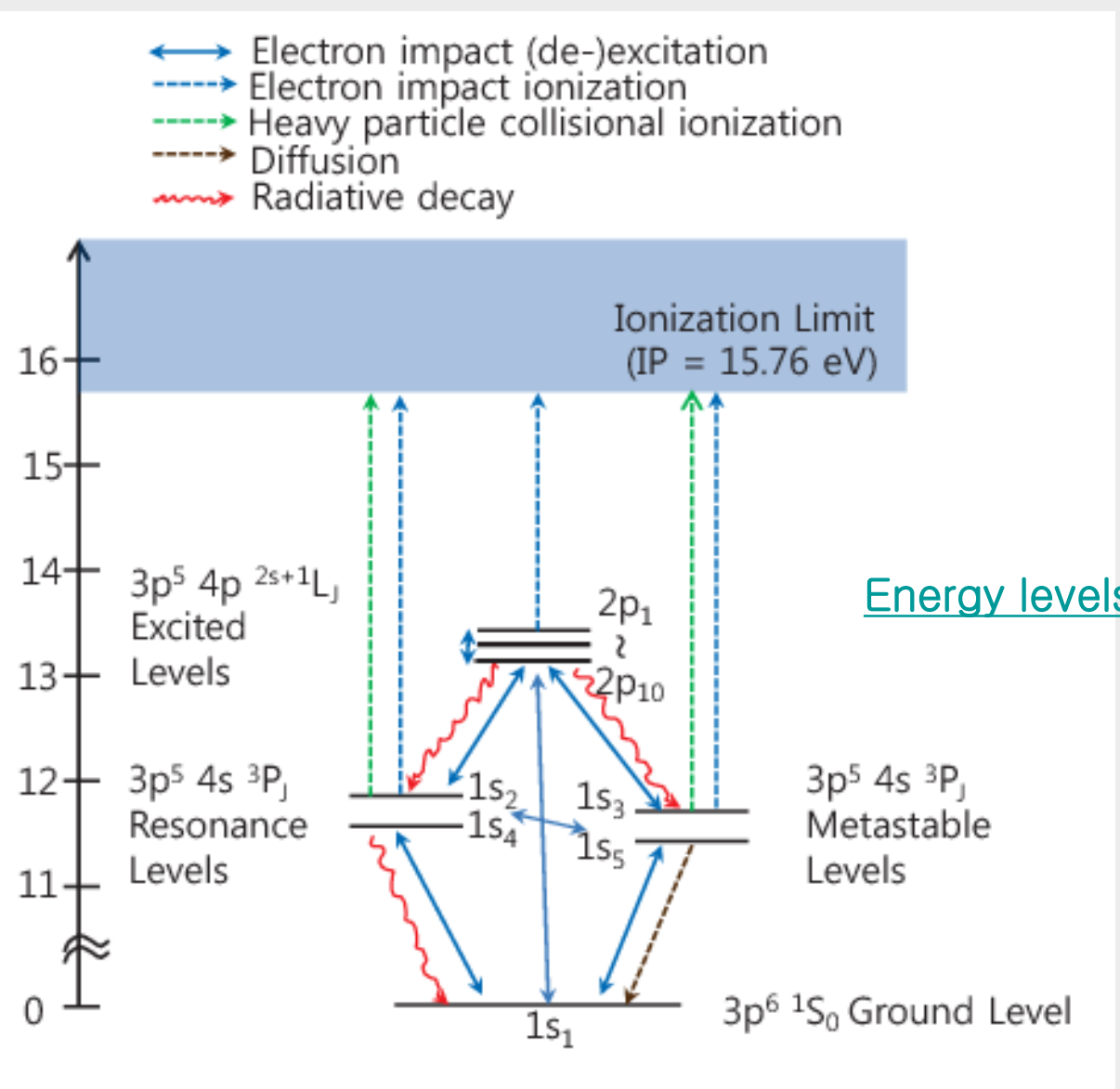
**Atomic data from the flexible atomic code (FAC)**

# OES and CR modeling in low temperature & low density plasmas

## Experimental setup



# CR model for Ar I plasma



**Transition wavelength (nm) and probability ( $10^8$  1/s) in parentheses**

Excited Levels	Resonance Levels		Metastable Levels	
	$1s_2$ (J=1)	$1s_4$ (J=1)	$1s_3$ (J=0)	$1s_5$ (J=2)
$2p_1$ (J=0)	750.39 (0.45)	667.73 (0.002)		
$2p_2$ (J=1)	826.45 (0.15)	727.29 (0.02)	772.42 (0.12)	696.54 (0.06)
$2p_3$ (J=2)	840.82 (0.22)	738.40 (0.08)		706.72 (0.04)
$2p_4$ (J=1)	852.14 (0.14)	747.12 (0.0003)	794.82 (0.19)	714.70 (0.006)
$2p_5$ (J=0)	858.01	751.47 (0.40)		
$2p_6$ (J=2)	922.45 (0.05)	800.62 (0.05)		763.51 (0.25)
$2p_7$ (J=1)	935.42 (0.01)	810.37 (0.25)	866.79 (0.02)	772.38 (0.05)
$2p_8$ (J=2)	978.45 (0.01)	842.46 (0.22)		801.48 (0.009)
$2p_9$ (J=3)				811.53 (0.33)
$2p_{10}$ (J=1)	1148.8 (0.002)	965.78 (0.05)	1047.0 (0.01)	912.30 (0.19)

● : Lines used for comparison of CRM with OES

Energy levels for Ar I

# CRM for low temperature plasma



## Steady state balance equation for excited levels

From the particle balance equation  $\frac{\partial n}{\partial t} + \nabla \cdot (n\mathbf{u}) = \frac{\delta n}{\delta t}$ ,  $n\mathbf{u} = -\nabla(D_a n)$

$$\frac{\partial N_i}{\partial t} - \nabla \cdot (\nabla D_a N_i) = \left( \frac{\delta N_i}{\delta t} \right)_{CR}, \quad \nabla \cdot (\nabla D_a N_i) \approx v_i^d N_i, \quad \frac{\partial N_i}{\partial t} = 0$$

In the weakly ionizing plasma conditions  $N_0 \alpha_I \gg n_+ \alpha_R$ ,  $n_+ \approx n_e$

$$\Rightarrow \sum_{j \neq i} n_e \alpha_{ji}^{ex} N_j + \sum_{j > i} \eta_{ji}(N_i) A_{ji} N_j = \sum_{j \neq i} n_e \alpha_{ij}^{ex} N_i + \sum_{j < i} \eta_{ij}(N_j) A_{ij} N_i + n_e \alpha_i^I N_i + \sum_j \alpha_{ij}^I N_i N_j + v_i^d N_i$$

**Populating terms**                           **Depopulating terms**

Nonlinear terms

The diagram illustrates the steady state balance equation for excited levels. It shows the equation split into three main categories: Populating terms, Depopulating terms, and Nonlinear terms. The Populating terms section contains terms involving excitation rates and electron density. The Depopulating terms section contains terms involving deexcitation rates and ion density. The Nonlinear terms section contains terms involving collisional rates and the product of electron and ion densities. Yellow arrows point from each category to a central 'Nonlinear terms' box, indicating that all three types of terms contribute to the nonlinear behavior of the plasma.

## Ground level population

$$p_{tot} = N_0 k_B T_g + n_+ k_B T_i + n_e k_B T_e \approx N_0 k_B T_g$$

$$N_0 \cong \frac{p_{tot}}{k_B T_g} \text{ (constant)}$$

## Diagnostics for plasma parameters

$$\text{Minimization of } \Delta(n_e, T_{eff}, R_{eff}, L_{eff}) = \sum \left( \frac{I_{ik}^{\text{CRM}} - I_{ik}^{\text{OES}}}{I_{ik}^{\text{OES}}} \right)^2, \quad I_{ik}^{\text{CRM}} = \frac{N_i \eta_{ik} A_{ik}}{\lambda_{ik}}$$

# Atomic data and plasma parameters for CRM of Ar I

## ❖ Gas temperature

Assumed to be close to room temperature (300K) for CCP at low pressures (p) and powers (P)

## ❖ Electron-impact excitation/deexcitation (EIE/DE)

$Ar + e \rightarrow Ar^* + e$  : BSR Quantum-mechanical calculation by O. Zatsariny & K. Bartschat  
in Lxcat DB (<https://nl.lxcat.net>)

## ❖ Electron-impact ionization

$Ar + e \rightarrow Ar^+ + 2e$  : Semi-empirical formula by L. Vriens (PRA 22, 940 (1980))

$$\alpha_i^{iz} (cm^3 s^{-1}) = \frac{9.56 \times 10^{-6} (k_B T_e)^{-1.5} \exp(-\Delta E_i / k_B T_e)}{(\Delta E_i / k_B T)^{2.33} + 4.38 (\Delta E_i / k_B T)^{1.72} + 1.32 (\Delta E_i / k_B T)} \quad \Delta E_i = E_{IP} - E_i$$

## ❖ Heavy particle collisional ionization

$Ar^* + Ar^* \rightarrow Ar + Ar^+ + e$  :  $\alpha_{rr}^{hiz} = 1.14 \times 10^{-14} \sqrt{\frac{16k_B T_g}{\pi M_{Ar}}}$ ,  $\alpha_{rm}^{hiz} = 2.1 \times 10^{-9}$ ,  $\alpha_{mm}^{hiz} = 1.2 \times 10^{-15}$

## ❖ Particle diffusion for metastable levels

$$D_m = D_{sc} \frac{n_{sc}}{n_0} \sqrt{\frac{T_g}{T_{sc}}} \quad v_m^d = \frac{1}{\tau_{eff}^d} = D_m \left[ \left( \frac{\pi}{L} \right)^2 + \left( \frac{2.405}{R} \right)^2 \right]$$

# EEDF and radiation trapping for CRM of Ar I

❖ We consider non-Maxwellian electron energy distribution as below:

$$\text{EEPF} : g_p(\varepsilon) = g_0 g_f(\varepsilon)$$

$$\text{EEDF} : g_f(\varepsilon) = \begin{cases} \exp\left(-\frac{\varepsilon}{T_e^{\text{low}}}\right) & (\varepsilon \leq \varepsilon_k) \\ \exp\left(-\frac{\varepsilon_k}{T_e^{\text{low}}} - \frac{\varepsilon - \varepsilon_k}{T_e^{\text{high}}}\right) & (\varepsilon > \varepsilon_k) \end{cases}$$

$T_e^{\text{low}}$ : electron temperature in the low-energy region

$T_e^{\text{high}}$ : electron temperature in high-energy region

$\varepsilon_k$ : knee energy

EEPF: electron energy probability function

EEDF: electron energy distribution function

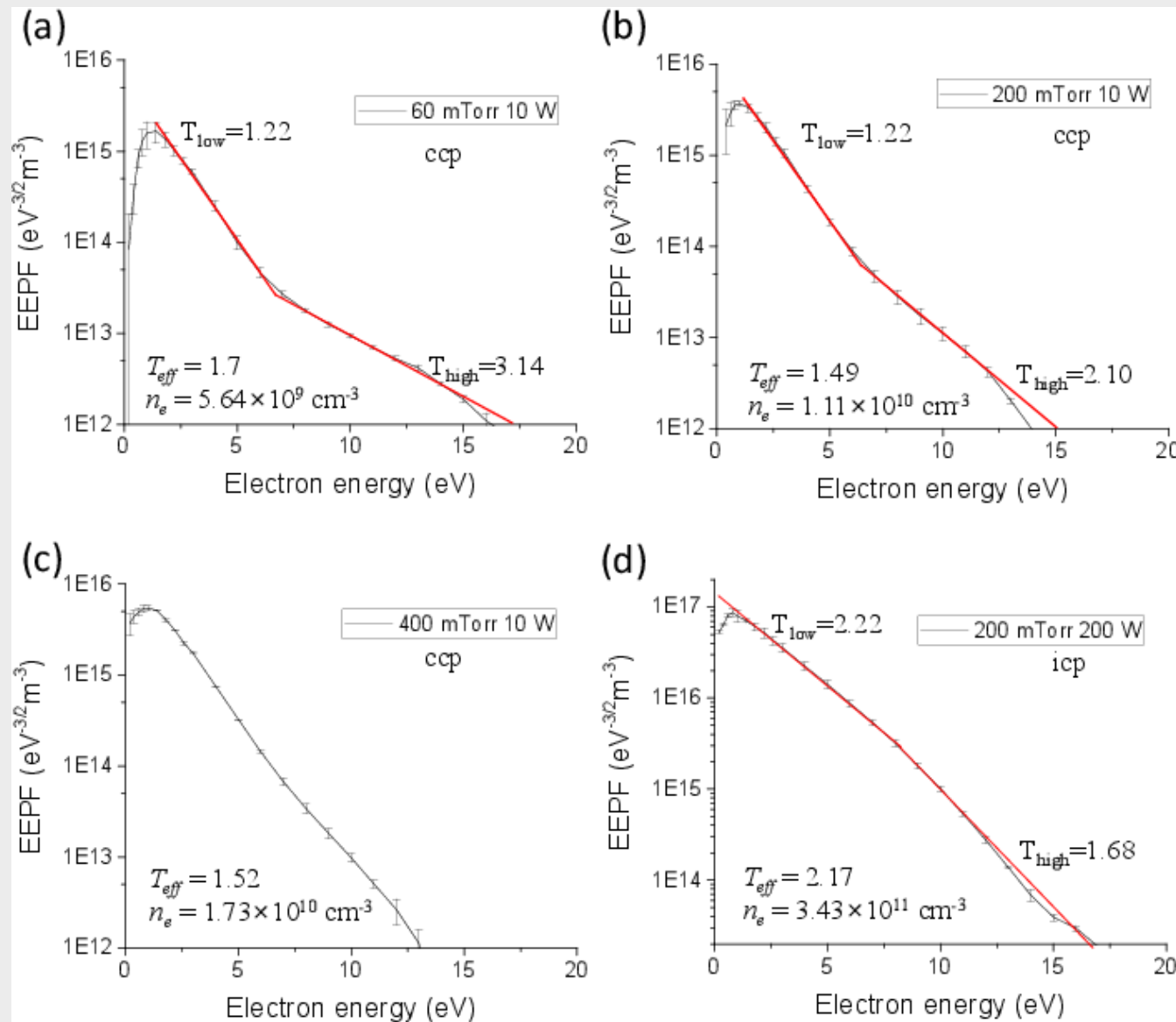
$$g_0 = \frac{n_e}{\int_0^\infty \sqrt{\varepsilon} g_f(\varepsilon) d\varepsilon}$$

❖ We also use an escape factor ( $\eta$ ) for finite cylinder

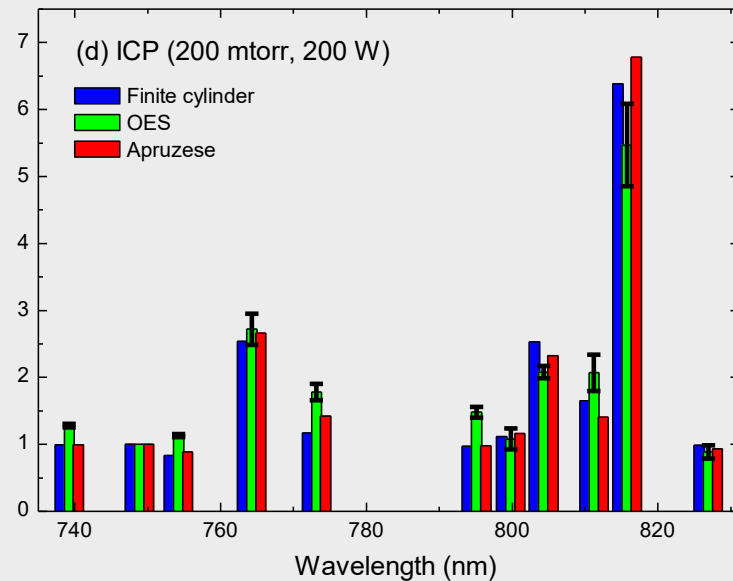
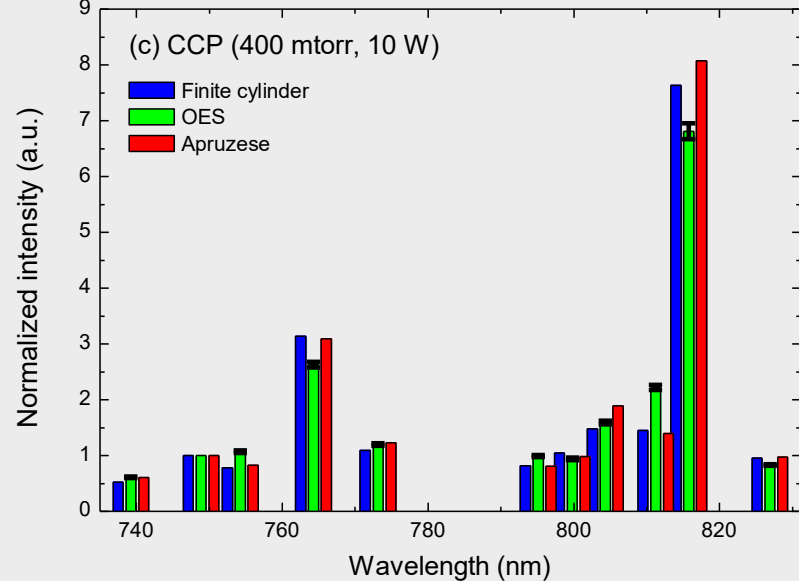
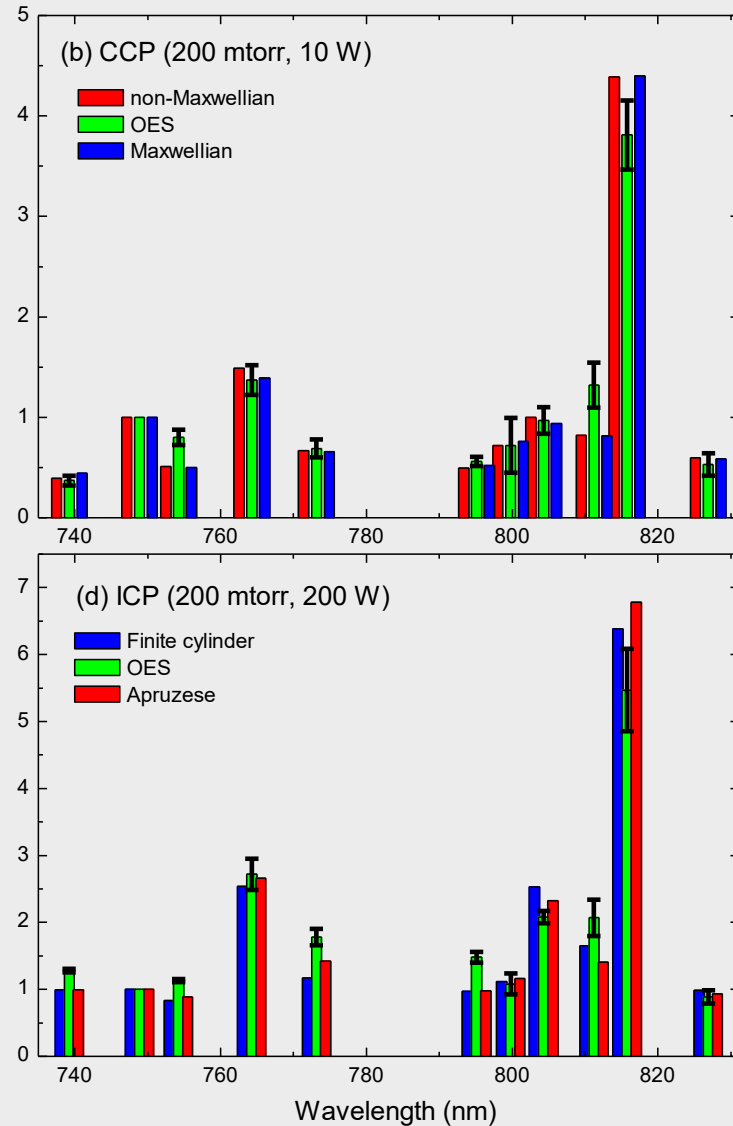
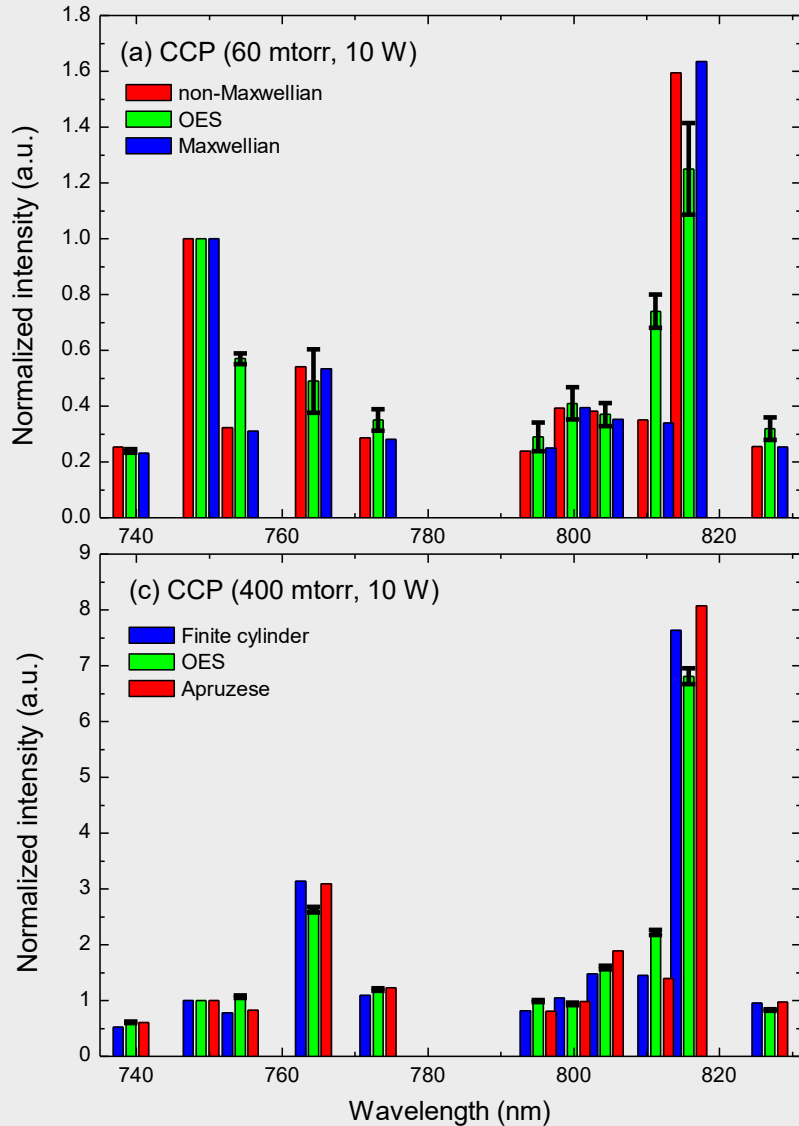
$$\begin{aligned} \eta(r, z) = & \frac{1}{\sqrt{\pi \log(k_0(L-z))} k_0(L-z)} \frac{1}{2\pi} \int_0^\pi d\psi \int_{(L-z)/q_0(\psi)}^\infty \frac{\xi d\xi}{(1+\xi^2)^2} & L: \text{plasma length} \\ & + \frac{1}{\sqrt{\pi} k_0} \frac{1}{2\pi} \int_0^\pi \frac{d\psi}{q_0(\psi) \sqrt{\log(k_0 q_0(\psi))}} \int_{-z/q_0(\psi)}^{(L-z)/q_0(\psi)} \frac{\xi d\xi}{(1+\xi^2)^2} & R: \text{plasma radius} \\ & + \frac{d\psi}{\sqrt{\pi \log(k_0 z)} k_0 z} \frac{1}{2\pi} \int_0^\pi d\psi \int_{z/q_0(\psi)}^\infty \frac{\xi d\xi}{(1+\xi^2)^2} & k_0: \text{absorption coefficient at the center} \end{aligned}$$

$$k_0 = \frac{\lambda^3 N_i g_j}{8\pi g_i} \sqrt{\frac{A_{ji} M}{2\pi k_B T_g}}$$

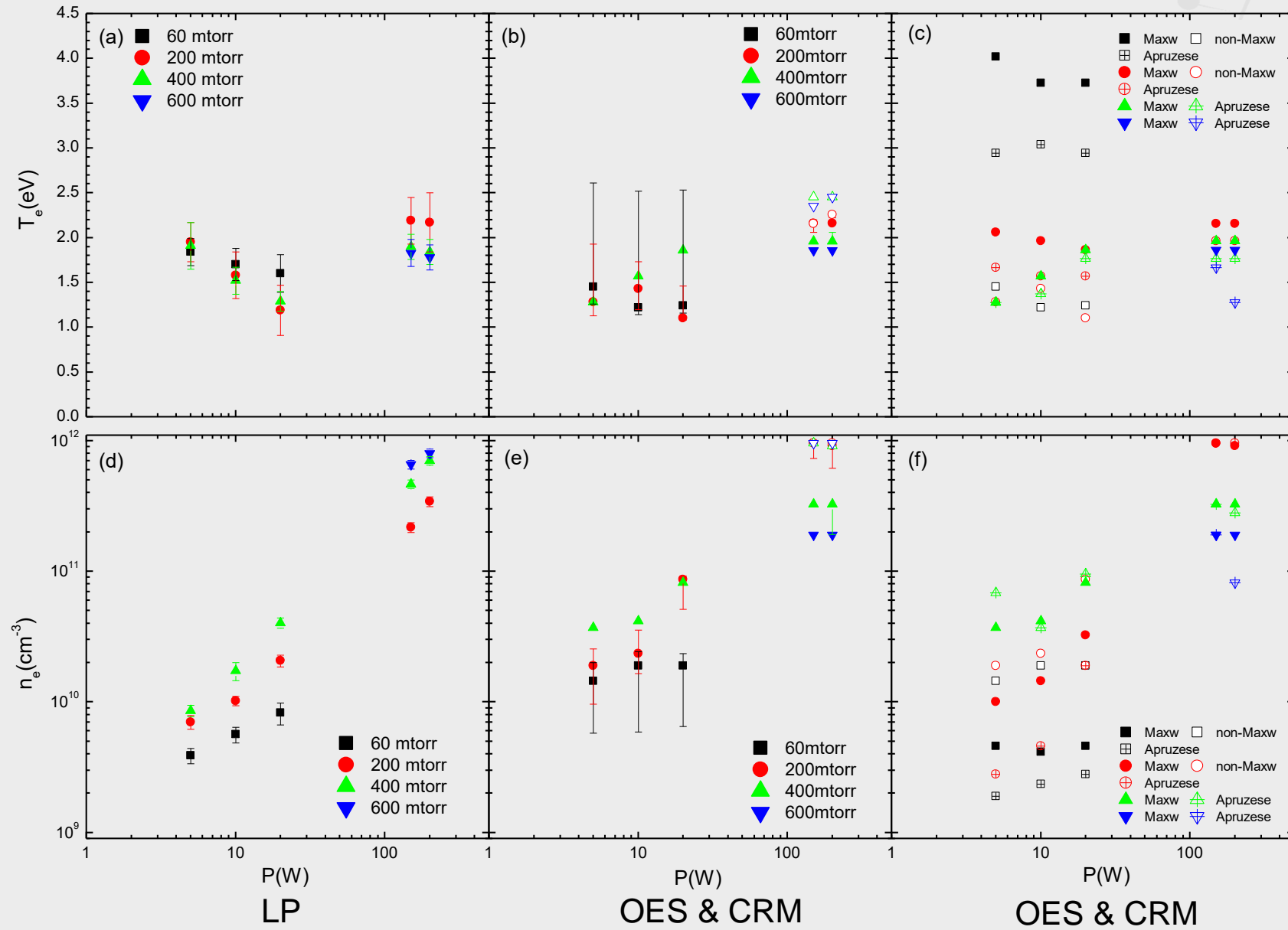
# EEPF for the CCP & the ICP of Ar



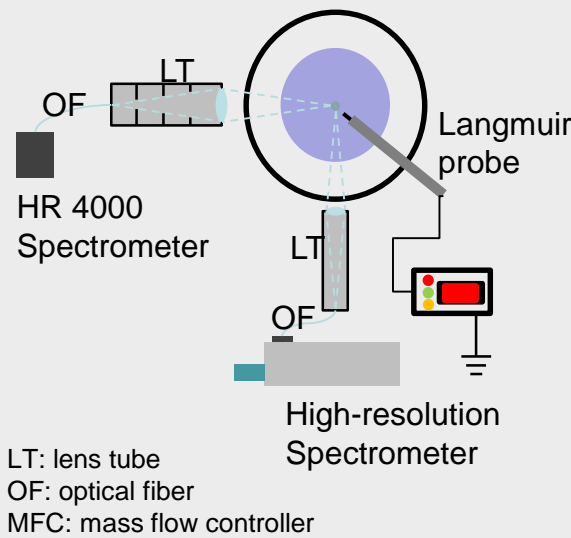
# Measured and modeled spectra for Ar I



# Diagnostics : OES with CRM vs. LP measurement

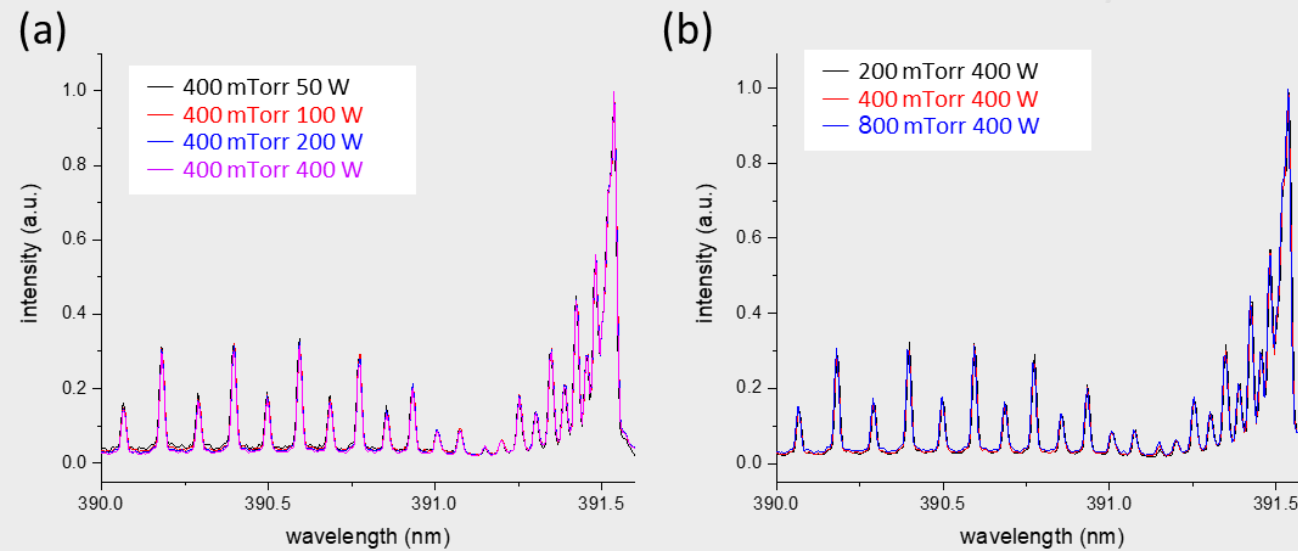


# OES for low temperature He plasma

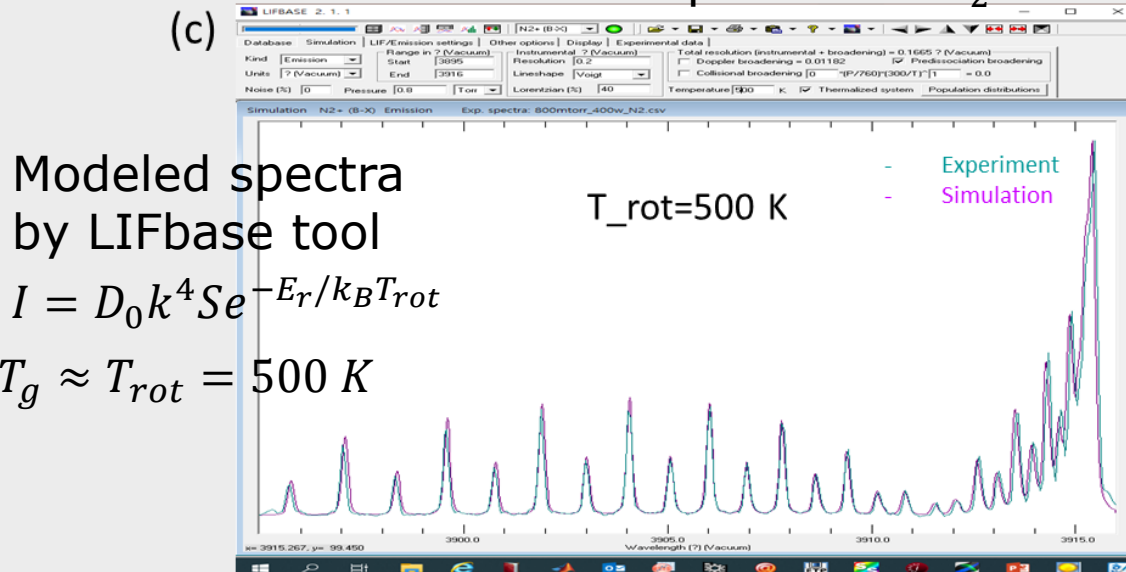


## Gas temperature

$T_g$  can be estimated with the  $N_2^+$  rotational temperature obtained from the emission spectra of the  $N_2^+$  transition  $B^2\Sigma_u^+, \nu = 0 \rightarrow X^2\Sigma_g^+, \nu' = 0$  by inserting  $\Rightarrow T_g \approx T_{rot} = 500 K$



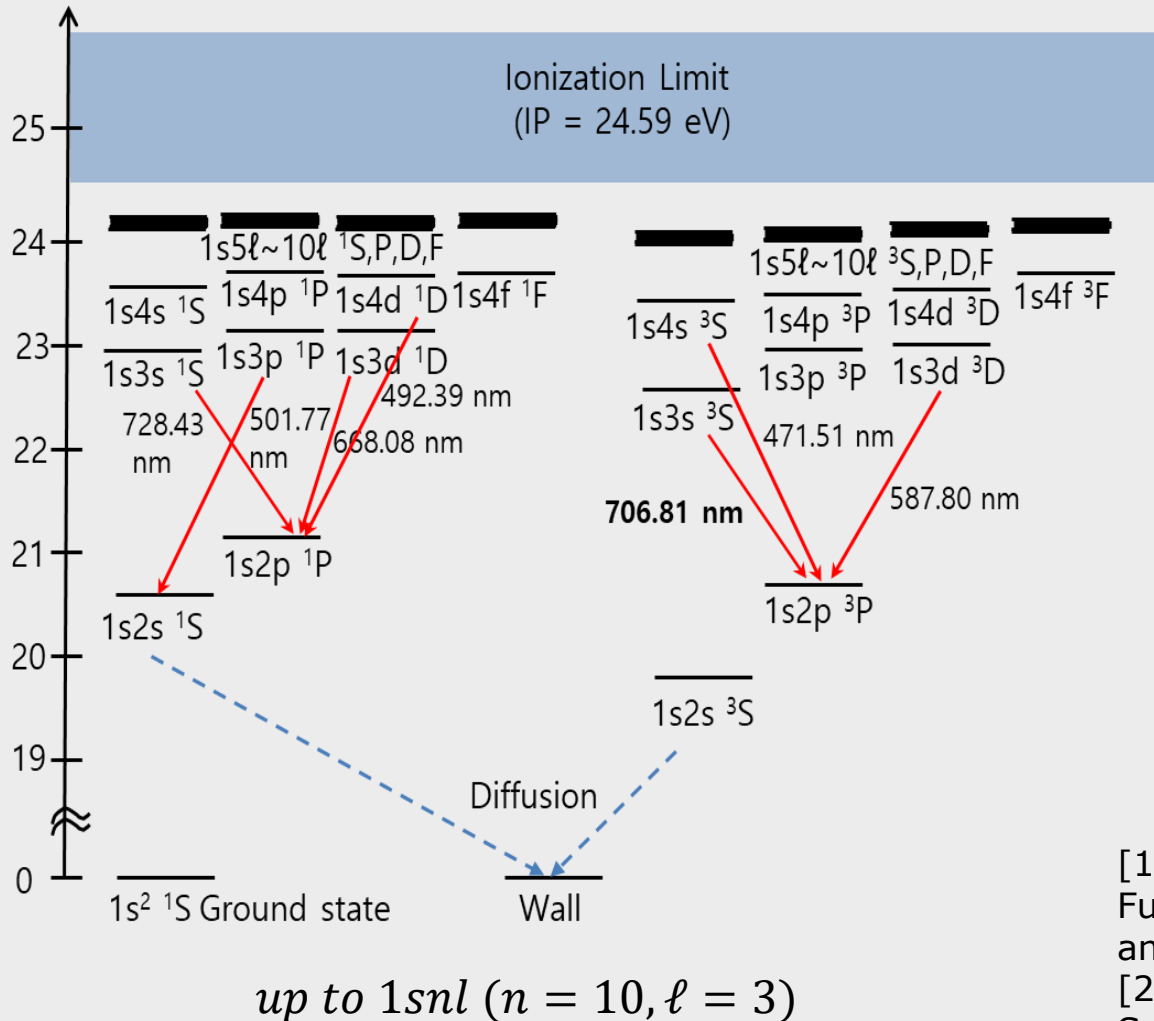
Measured spectra for  $N_2^+$



# CRM for low temperature He I plasma



## Energy levels



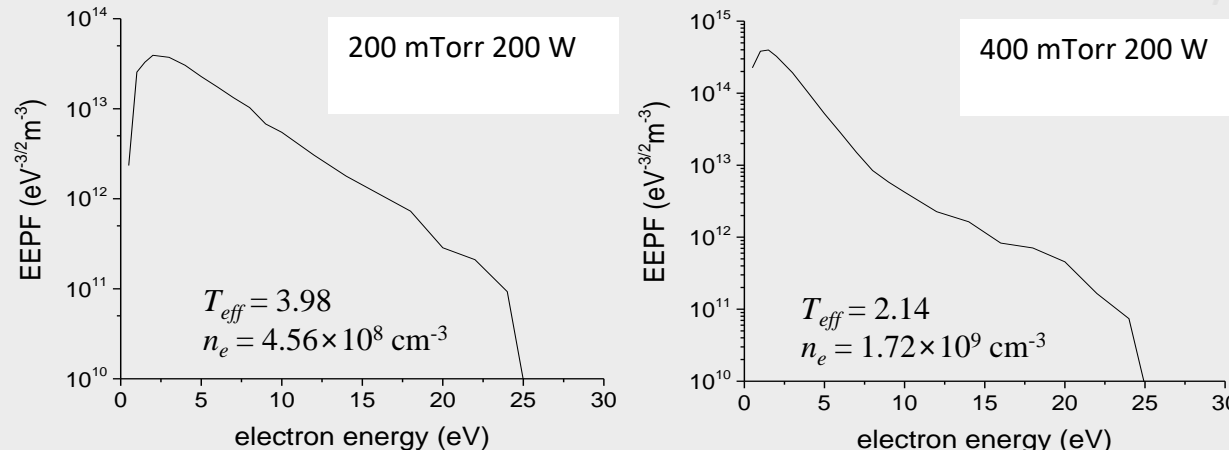
## Kinetic processes

- $\text{He} + \text{e} \rightarrow \text{He}^* + \text{e}$        $\alpha_{ij}^{ex}$  [1]
  - $\text{He} + \text{e} \rightarrow \text{He}^+ + 2\text{e}$        $\alpha_i^I$  [1]
  - $\text{He}^* \rightarrow \text{He} + h\nu$        $\lambda_{ij}, A_{ij}$  [2]
  - $\text{He}(1s2\ell) + \text{He}(1s2\ell') \rightarrow \text{He}^+ + \text{He} + \text{e}$        $\alpha_{ij}^I$
- $$2.9 \times 10^{-9} (T_g/300)^{1/2} (\text{cm}^3/\text{s})$$
5.  $\text{He}(1s2s) \rightarrow \text{to wall}$        $v_i^d$
- $$v_i^d = D_a \left( \left( \frac{2.405}{R_{eff}} \right)^2 + \left( \frac{\pi}{L_{eff}} \right)^2 \right),$$
- $$D_a = 8.992 \times 10^{-2} \frac{T_g^{3/2}}{p} (\text{cm}^3/\text{s})$$

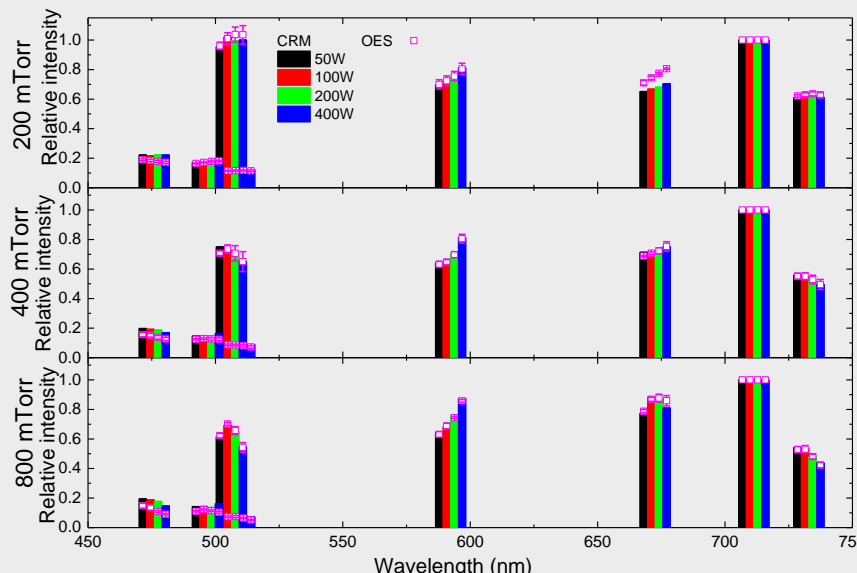
- [1] Y. Ralchenko, R. K. Janev, T. Kato, D. V. Fursa, I. Bray, F. J. de Heer, Atomic Data and Nuclear Data Tables 94 (2008) 603.  
[2] G.W.F Drake, D.C. Morton, Astrophys. J. Suppl. Series 170 (2007) 251.

# OES & CRM vs. LP measurement for low temperature He plasma

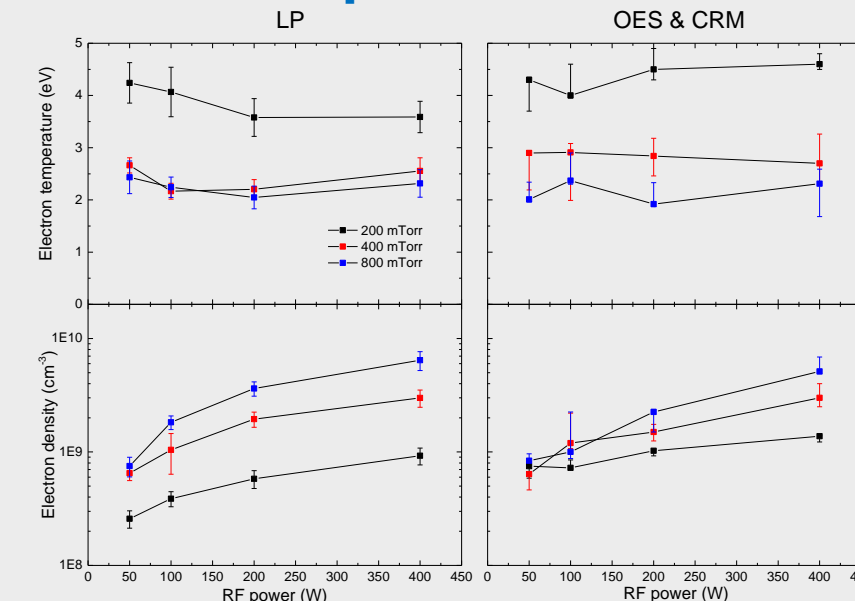
## Non-Maxwellian electron energy distribution



OES and CR modeling spectra



Electron temperature and density

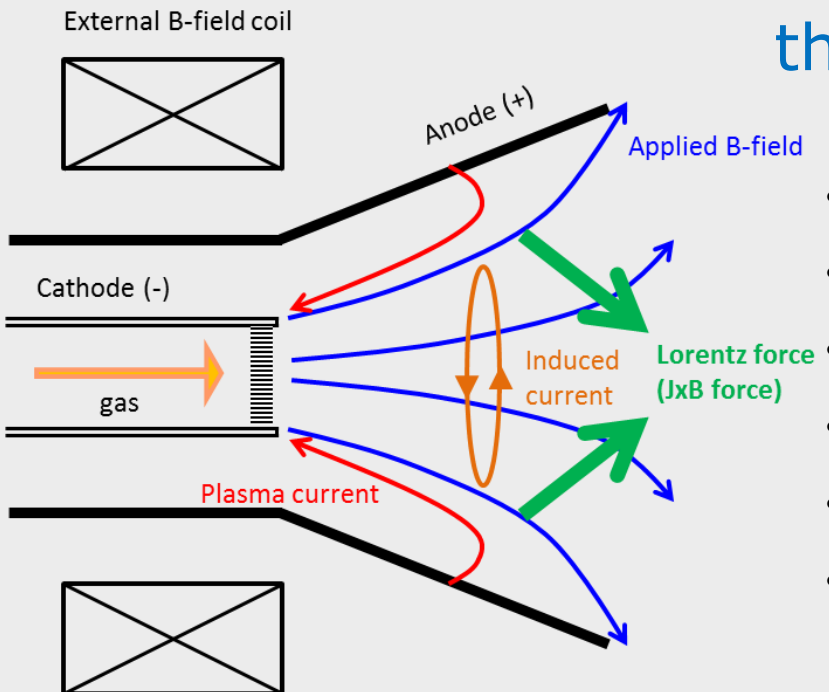


# KAERI Plasma Beam Irradiation Facility (PBIF)

## Motivation of the construction

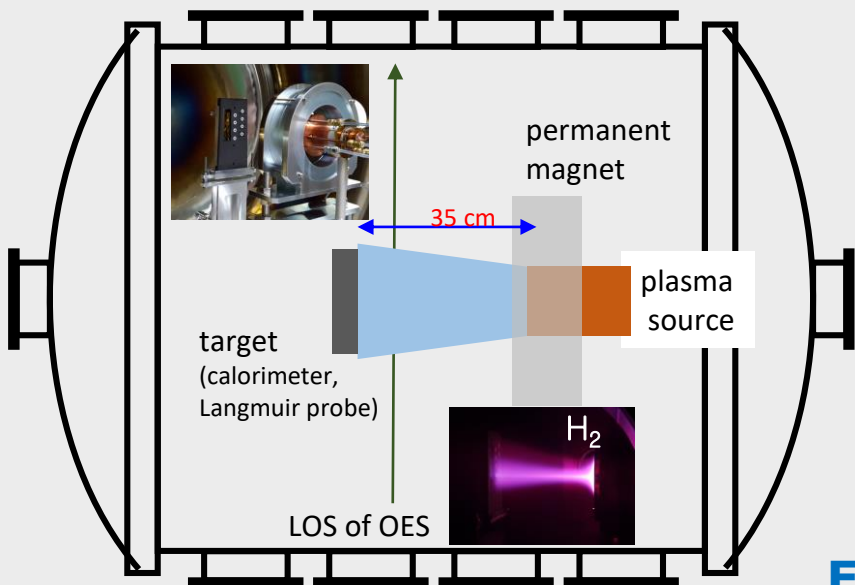
In order to develop divertor materials and cooling techniques resisting **high heat** and **particle fluxes** (heat flux of  $10 \text{ MW/m}^2$  and particle flux of  $10^{24} / \text{m}^2\text{s}$  will come in ITER and much larger heat and particle fluxes will come in DEMO), we have constructed **lab-scale** divertor plasma simulator

## Applied field-magnetoplasmadynamic (AF-MPD) thruster concept

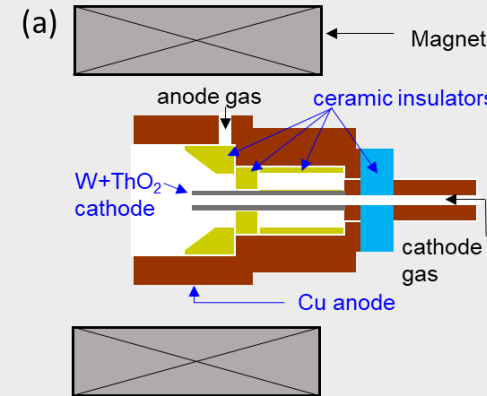


- | type I / type II  | type I / type II  |
|---|---|
| • Anode radius = $4/2 \text{ cm}$ , cathode radius = $0.6/0.4 \text{ cm}$ | • Anode material: Cu, cathode material: W+ThO <sub>2</sub> (2%) |
| • Insulating material : ceramic ( $\text{Al}_2\text{O}_3$ )               | • Sustain power supply : DC 10-20 kW                            |
| • External B-field: 0.17 T (NdFeB permanent magnet)                       | • Both anode & cathode can be water-cooled                      |

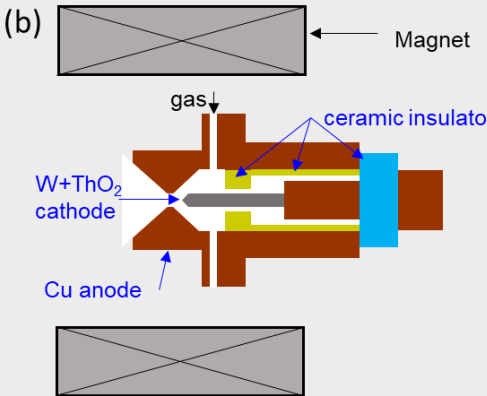
# KAERI AF-MPD PBIF



## Plasma source schemes

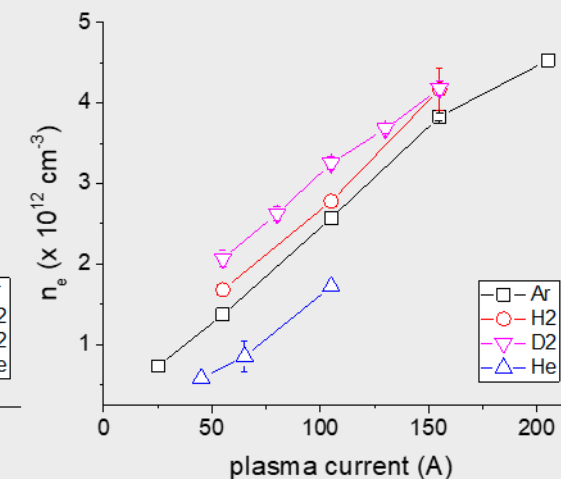
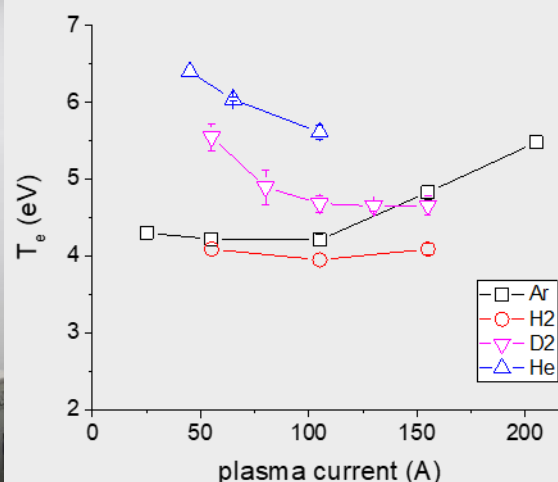


Type I for Ar



Type II for H<sub>2</sub>,D<sub>2</sub>,He

## Electron temperature and density by LP



# CR modeling for H/D plasma



## Considered processes

$H(n \geq 1) + e \leftrightarrow H(n' > n) + e$	(1) [1]	[1] R. K. Janev, D. Reiter and U Samm, Collision processes in low-temperature hydrogen plasmas, Report JUEL-4105 (2003).
$H(n \geq 1) + e \leftrightarrow H^+ + 2e$	(2) [1]	
$H(n \leq 40) \rightarrow H(n' < n) + h\nu$	(3) [1]	[2] R. K. Janev et al., Elementary processes in Hydrogen-Helium plasmas, (Berlin: Springer 1987)
$H^+ + e \rightarrow H(n \leq 40) + h\nu$	(4) [1]	
$H_2 + e \rightarrow H(n = 1) + H(n' \leq 3) + e$	(5) [2]	[3] W. L. Wiese, and J. R. Fuhr, Accurate atomic transition probabilities for H, He, Li, J. Phys.. Chem. Ref. Data <b>38</b> 565 (2009).
$H_2 + e \rightarrow 2H(n = 2) + e$	(6) [2]	
$H_2 + e \rightarrow H^+ + H(n = 1) + e$	(7) [1]	[4] P. del Mazo-Sevillano, ..., D.-H. Kwon, O. Roncero, Molecular physics e2183071
$H_2 + e \rightarrow H_2^+ + 2e$	(8) [1]	
$H_2^+ + e \rightarrow H(n = 1) + H(n' \geq 2)$	(9) [3]	❖ The cross sections for electron collisions and radiative transitions of D species were used by those of H species. The heavy particle collision cross section of D species was from the ab-initio calculation for D [4]. The mass effect for rate coefficients and mobility of D were taken into account.
$H_2^+ + e \rightarrow H^+ + H(n \leq 2) + e$	(10) [3]	
$H_2^+ + e \rightarrow 2H^+ + e$	(11) [3]	
$H_2^+ + e \rightarrow H_2^* \rightarrow H(n = 1) + H(n' \geq 2)$	(12) [1]	
$H_3^+ + e \rightarrow 3H(n = 1)$	(13) [3]	
$H_3^+ + e \rightarrow H_2 + H(n = 2)$	(14) [3]	
$H_3^+ + e \rightarrow H^+ + 2H(n = 1) + e$	(15) [3]	
$H_2^+ + H_2 \rightarrow H(n = 1) + H_3^+$	(16) [4]	

$$\alpha(T_{12}) = \frac{4}{\sqrt{\pi} v_{T_{12}}^3} \int_0^\infty \sigma(v_{12}) \exp\left(\left(v_{12}/v_{T_{12}}\right)^2\right) v_{12}^3 dv_{12}$$

$$T_{12} = (m_2 T_1 + m_1 T_2)/(m_1 + m_2)$$

$$v_{T_{12}} = \sqrt{2(m_1 + m_2)T_{12}/m_1 m_2}$$

# CRM for H/D plasma



**For atomic levels  $n_i$  ( $i = 1 - 40$ )**

$$D_{AH^+} = T_e K_1^0 \left( \frac{760}{p} \frac{T_m}{273} \right)$$

$$p = n_{H_2} T_m$$

$$K_1^0 = 15.9 \text{ (H}^+), 11.2 \text{ (D}^+) \text{ (cm}^2 V^{-1} s^{-1}\text{)}$$

$$D_{AH^+}: D_{AH_2^+}: D_{AH_3^+} = 1: \frac{\sqrt{2}}{\sqrt{3}}: \frac{\sqrt{5}}{3}$$

$$\begin{aligned} \frac{dn_i}{dt} = & \sum_{j>i}^{40} \eta_{ji} A_{ji} n_j - \left( \sum_{j*Q}{V} + \frac{\gamma}{\tau} \delta_{i1} \right) n_i + \\ & n_e \left( \sum_{j \neq i} \beta_{1,ji} n_j - \sum_{j \neq i} \beta_{1,ij} n_i - \beta_{2i} n_i + \beta_{4i} n_{H^+} \right) + \\ & n_e (\beta_{5i} + \beta_6 \delta_{i2} + \beta_7 \delta_{i1}) n_{41} + n_e (\beta_{9i} + \beta_{10i} + \beta_{12i}) n_{42} + \\ & n_e (\beta_{13} \delta_{i1} + \beta_{14} \delta_{i2} + \beta_{15} \delta_{i1}) n_{43} + n_{41} \beta_{16} \delta_{i1} n_{42} + \\ & \left( \sum_{j=42}^{43} \varsigma_{aj} \left(\frac{\mu}{R}\right)^2 D_{Aj} n_j + \varsigma_{aD^+} \left(\frac{\mu}{R}\right)^2 D_{AH^+} n_{H^+} \right) \delta_{i1} \end{aligned}*$$

$$\tau = 2R/v_{th}$$

$$v_{th} = 2 \sqrt{\frac{2T_a}{\pi M_H}}$$

$$\mu = 2.405$$

**For molecule and ions  $n_i$  ( $i=41,42,43$  for  $H_2$ ,  $H_2^+$ ,  $H_3^+$ )**

$$\begin{aligned} \frac{dn_i}{dt} = & \delta_{i41} \left( n_e \beta_{14} n_{43} + \frac{Q_{in}}{V} \times 4.48 \times 10^{17} + \frac{\gamma'}{\tau} n_1 + \sum_{j=42}^{43} \varsigma_{mj} \left(\frac{\mu}{R}\right)^2 D_{Aj} n_j + \varsigma_{mH^+} \left(\frac{\mu}{R}\right)^2 D_{AH^+} n_{H^+} \right) \\ & - \delta_{i41} n_e (\beta_5 + \beta_6 + \beta_7 + \beta_8) n_i - \delta_{i42} n_e (\beta_9 + \beta_{10} + \beta_{11} + \beta_{12}) n_i - \\ & \delta_{i43} n_e (\beta_{13} + \beta_{14} + \beta_{15}) n_i + \delta_{i42} (n_e \beta_8 - n_{41} \beta_{16}) n_i + \\ & n_{41} \beta_{16} \delta_{i43} n_{42} - \delta_{i41} \beta_{16} n_{42} n_i - \frac{Q}{V} n_i - (1 - \delta_{i41}) \left(\frac{\mu}{R}\right)^2 D_{Ai} n_i \end{aligned}$$

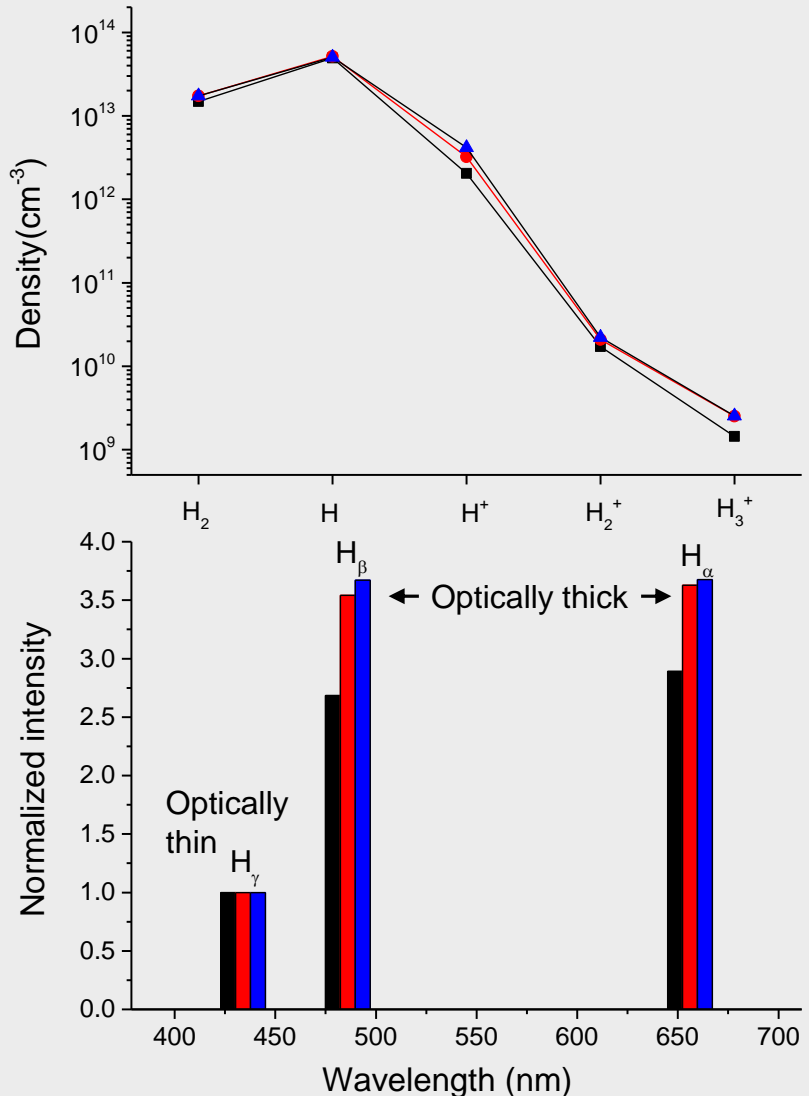
**Quasi neutrality condition** for  $H^+$  ion  $n_{H^+}$  :  $n_e = n_{H^+} + n_{H_2^+} + n_{H_3^+}$

rather than **pressure balance equation** :

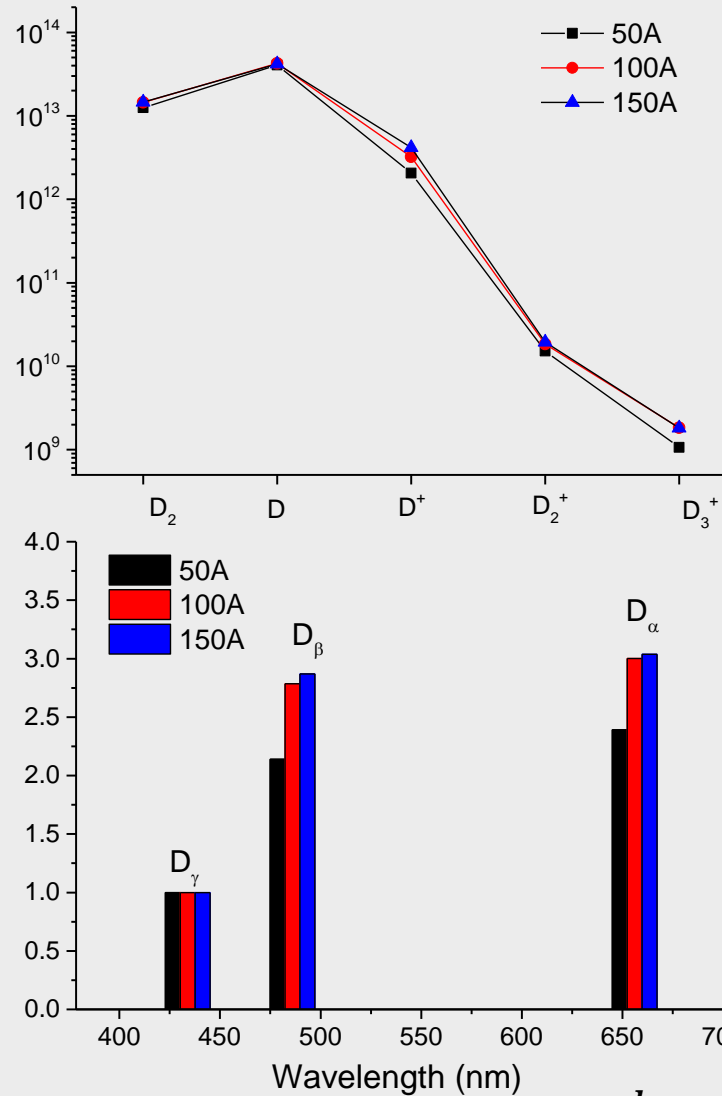
$$p_{tot} = n_m k_B T_m + k_B T_a (\sum_{j=1}^{40} n_j + n_{H^+}) + n_e k_B T_e + n_m k_B (n_{H_2^+} + n_{H_3^+})$$

P. del Mazo-Sevillano, ..., D.-H. Kwon, O. Roncero, “Vibrational, non-adiabatic and isotopic effects in the dynamics of the  $H_2 + H_2^+ \rightarrow H_3^+ + H$  reaction: application to plasma modeling”, Molecular physics e2183071 (2023)

# Results for H/D CRM



$H \rightarrow D$ ,  $k_0 \uparrow \eta \downarrow$



$$k_0 = \frac{\lambda^3 N_i g_j}{8\pi g_i} \sqrt{\frac{A_{ji} M}{2\pi k_B T_g}}$$

$T_m = 300\text{K}$ ,  
 $T_a = 600\text{K}$ ,  
 $R_{eff} = 40\text{ cm}$ ,

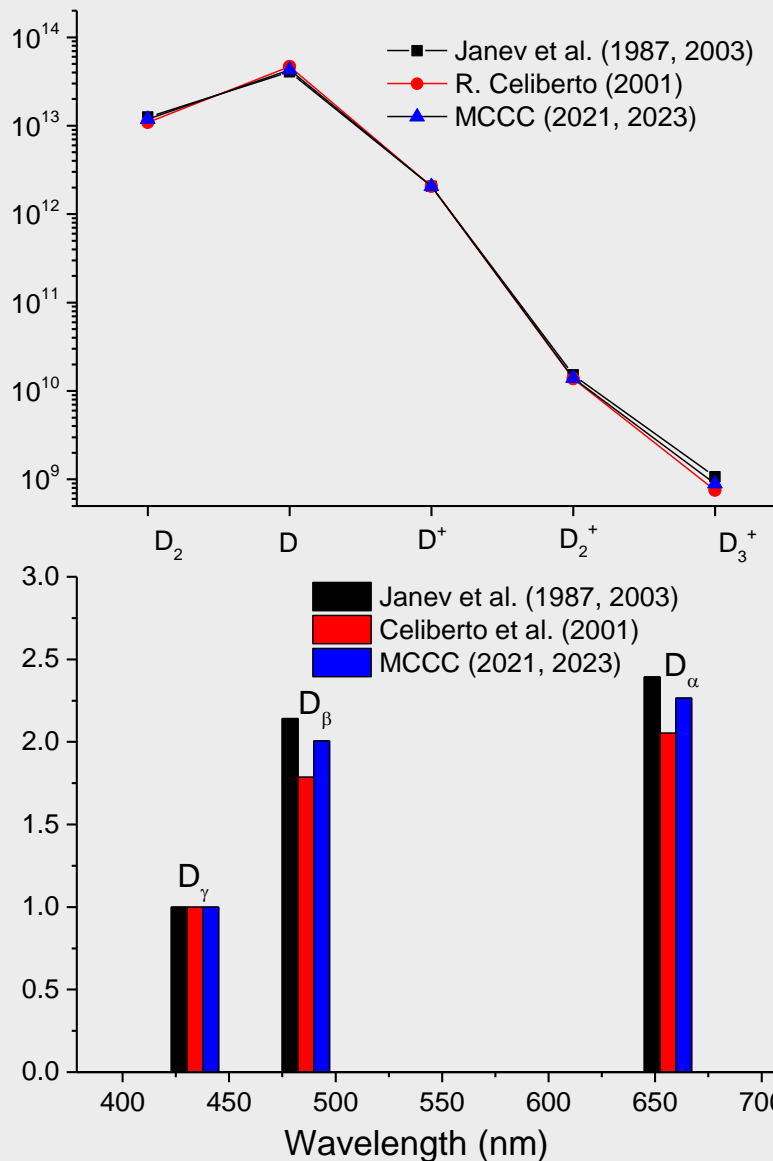
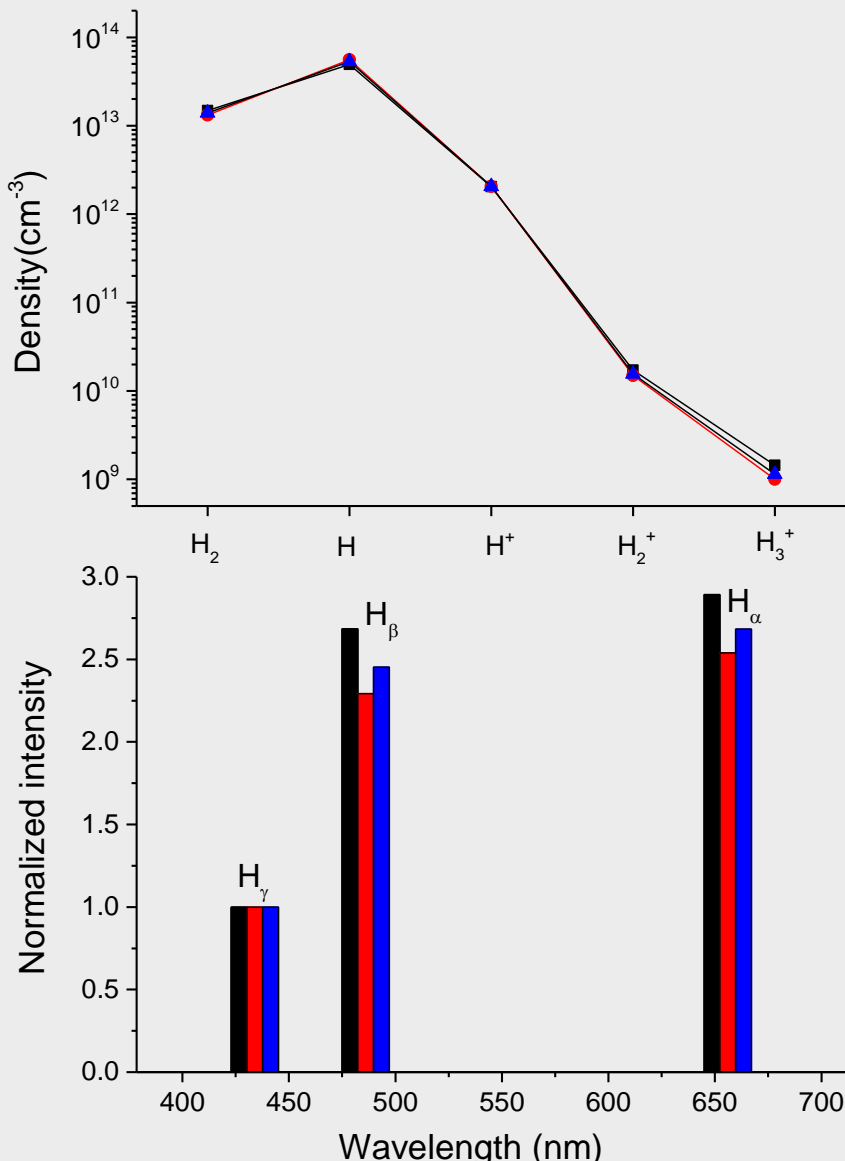
$T_e = 5.55\text{ (50A)}$ ,  
 $4.68\text{ (100A)}$ ,  
 $4.66\text{ (150A) eV}$

$n_e = 2.07\text{ (50A)}$ ,  
 $3.25\text{ (100A)}$ ,  
 $4.18\text{ (150A)}$ ,  
 $\times 10^{12}\text{ (cm}^{-3})$

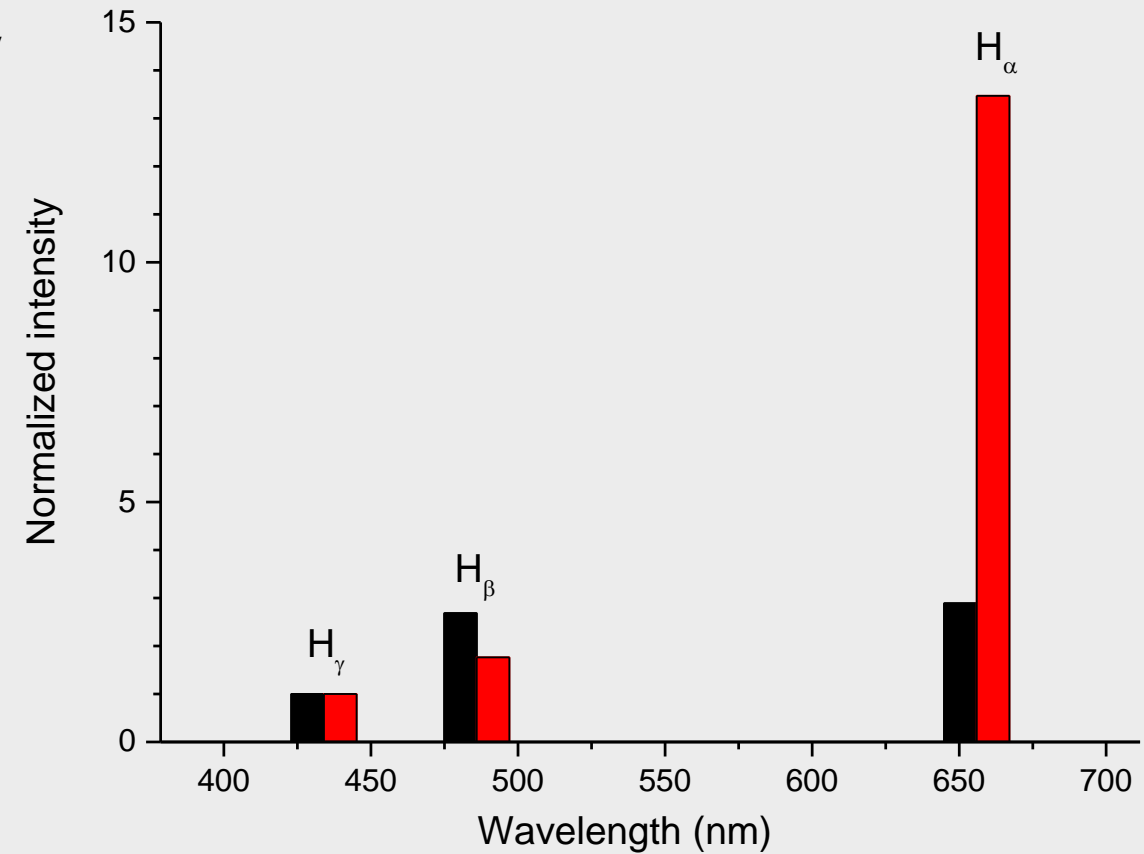
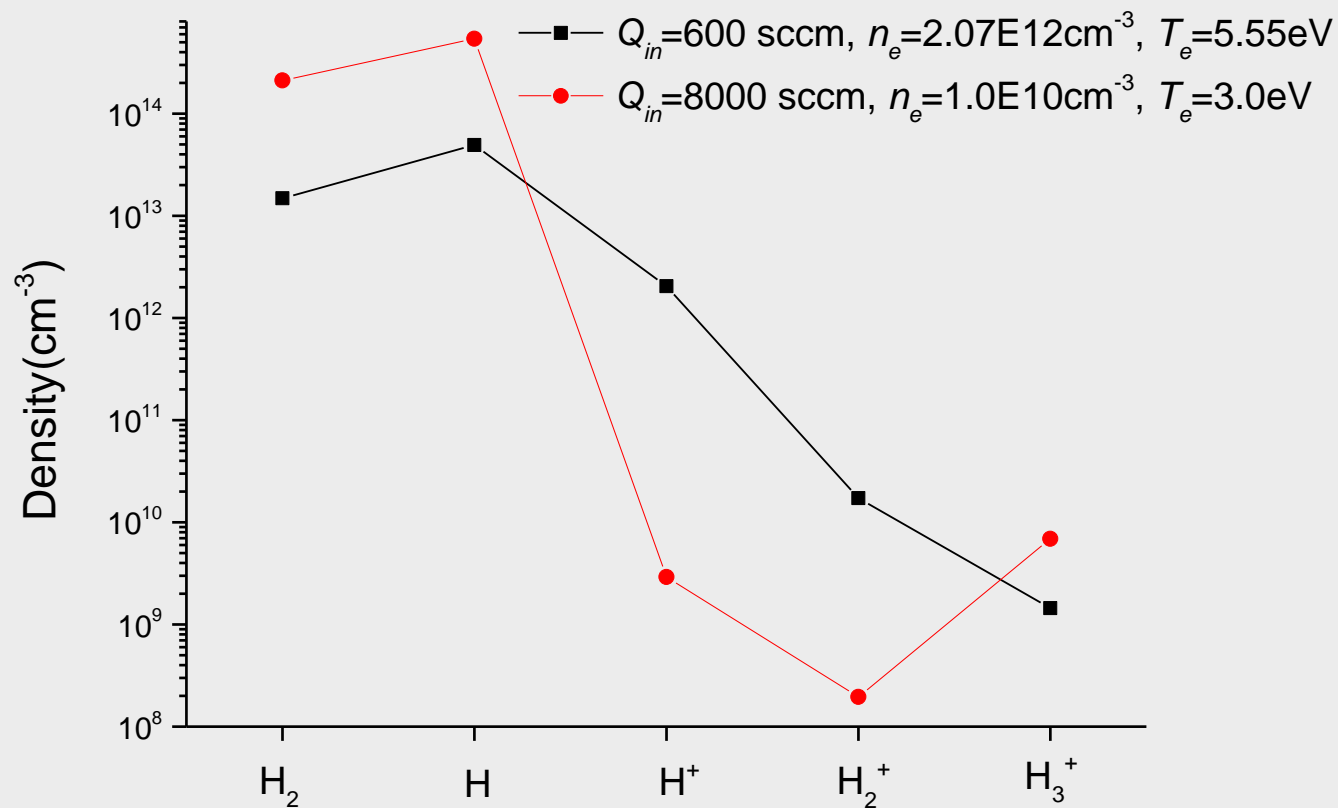
$Q_{in} = 600\text{ sccm}$ ,  
 $Q = 4800\text{ lps}$ ,

$V = 2.64 \times 10^6\text{ cm}^3$ ,  
 $R = 75\text{ cm}$

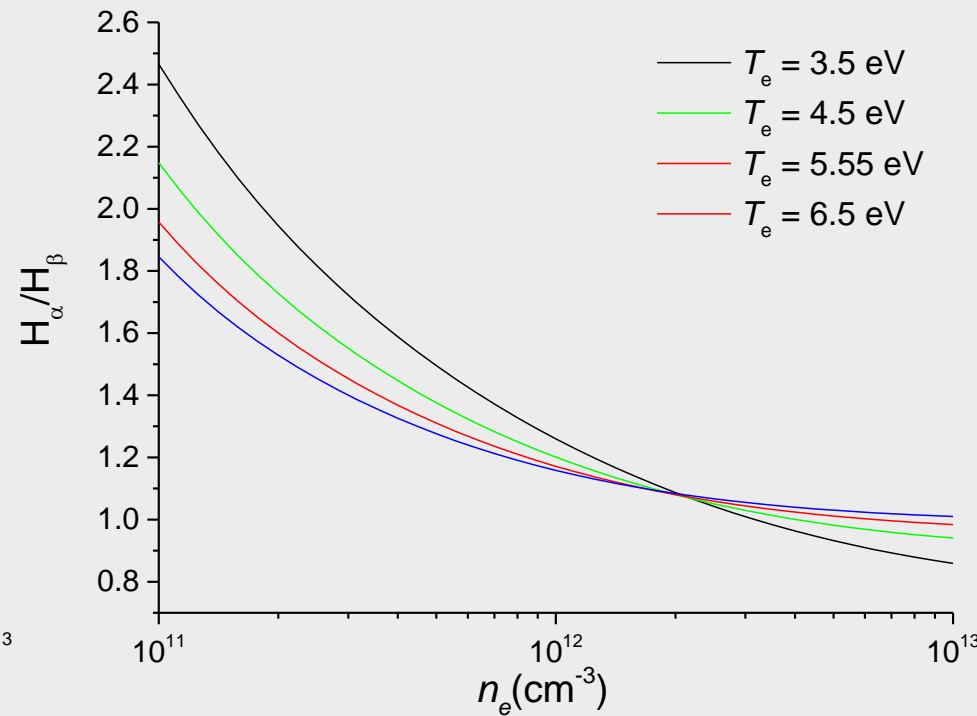
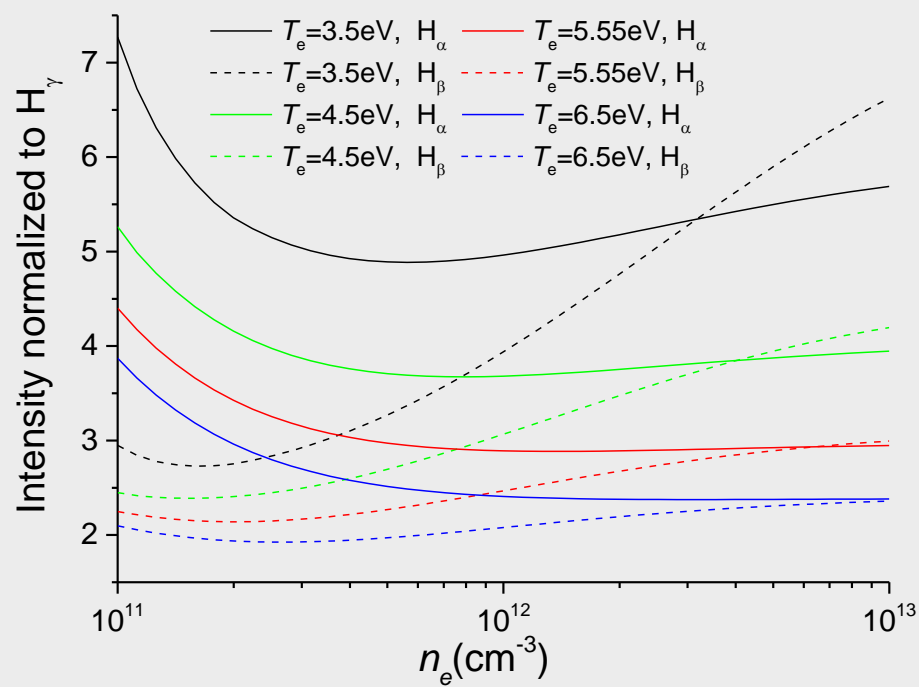
# Resulting populations and spectra for different atomic and molecular data sources



# $\text{H}_3^+$ dominant case

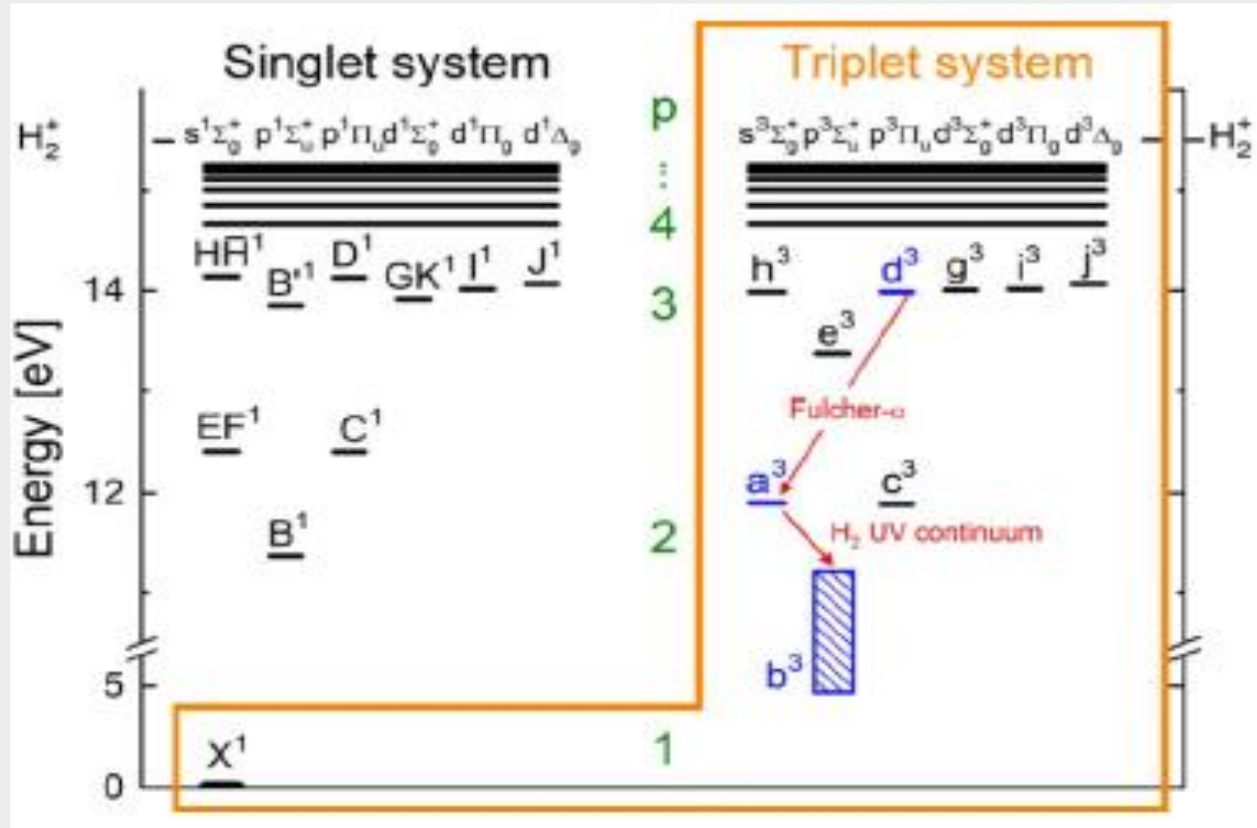


# Sensitivity to plasma parameters $n_e$ and $T_e$



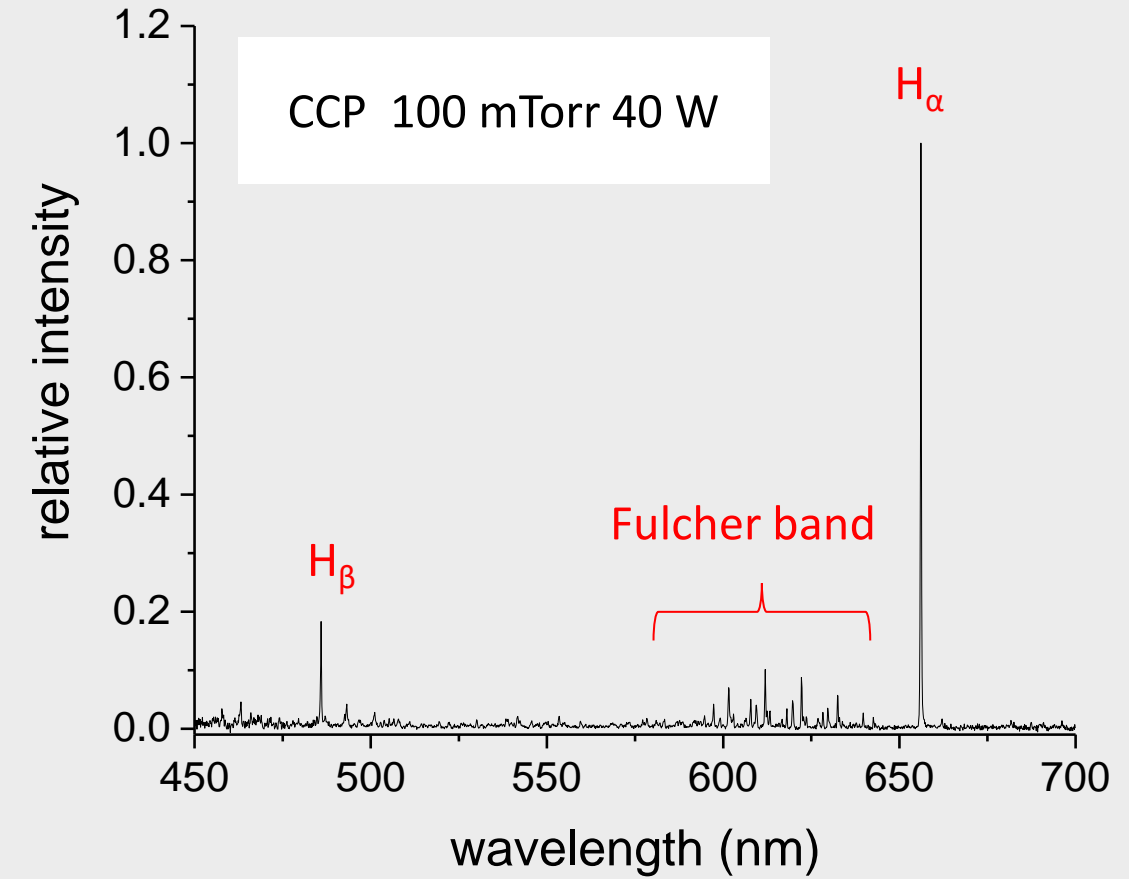
# CR modeling for vibrational states of H molecules : Future works

Energy level diagram of  $\text{H}_2$

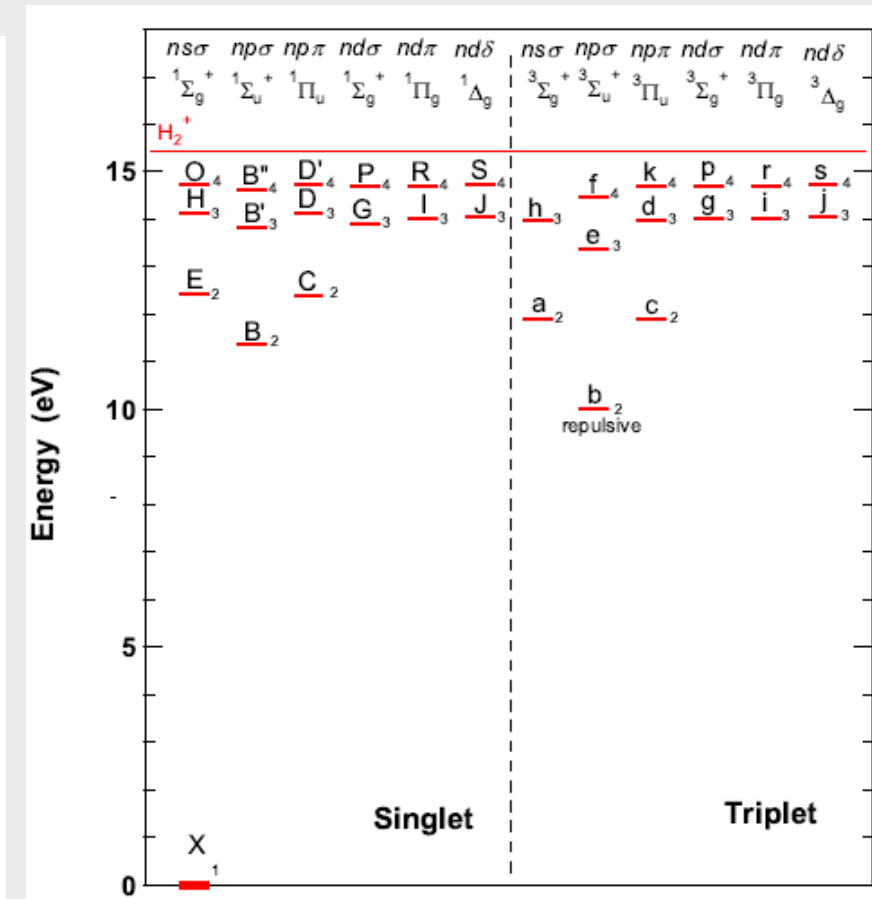
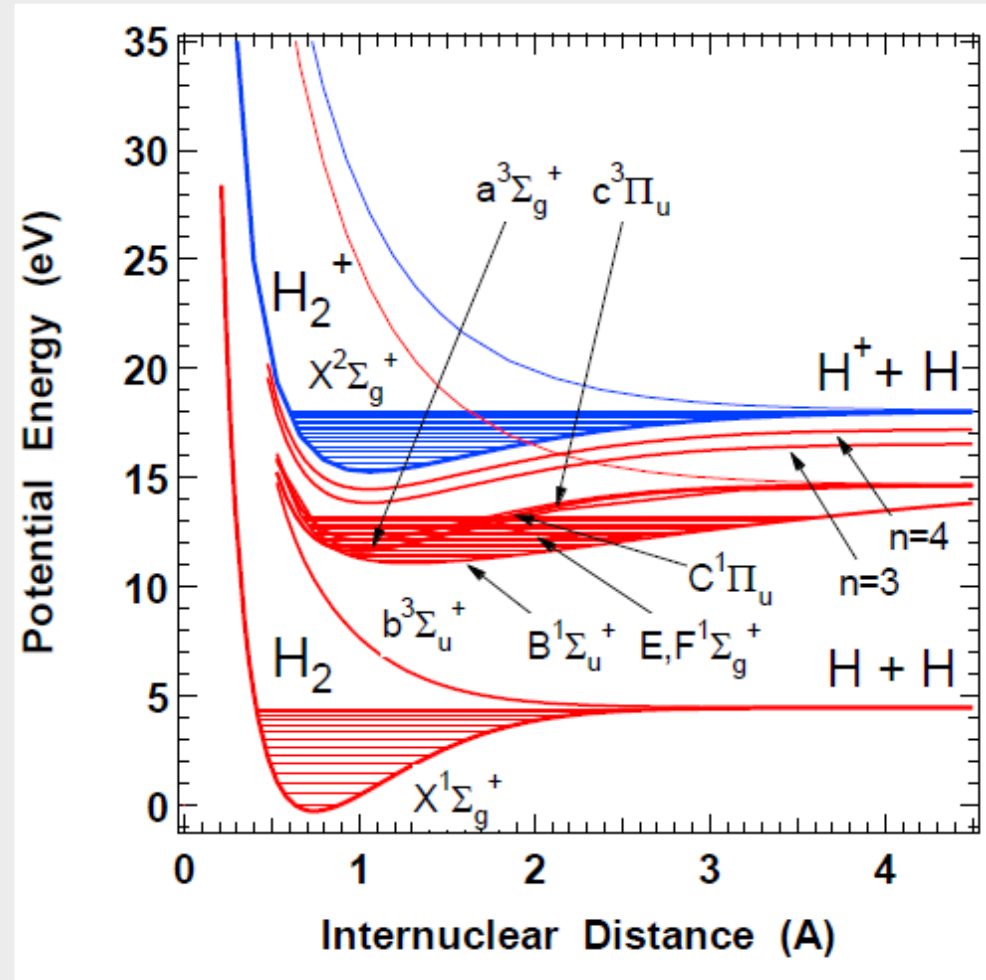


Ref. D. Wunderlich et al., J. Phys. D: Appl. Phys. **54** 115201 (2016)

CR modeling for the measured molecular spectra



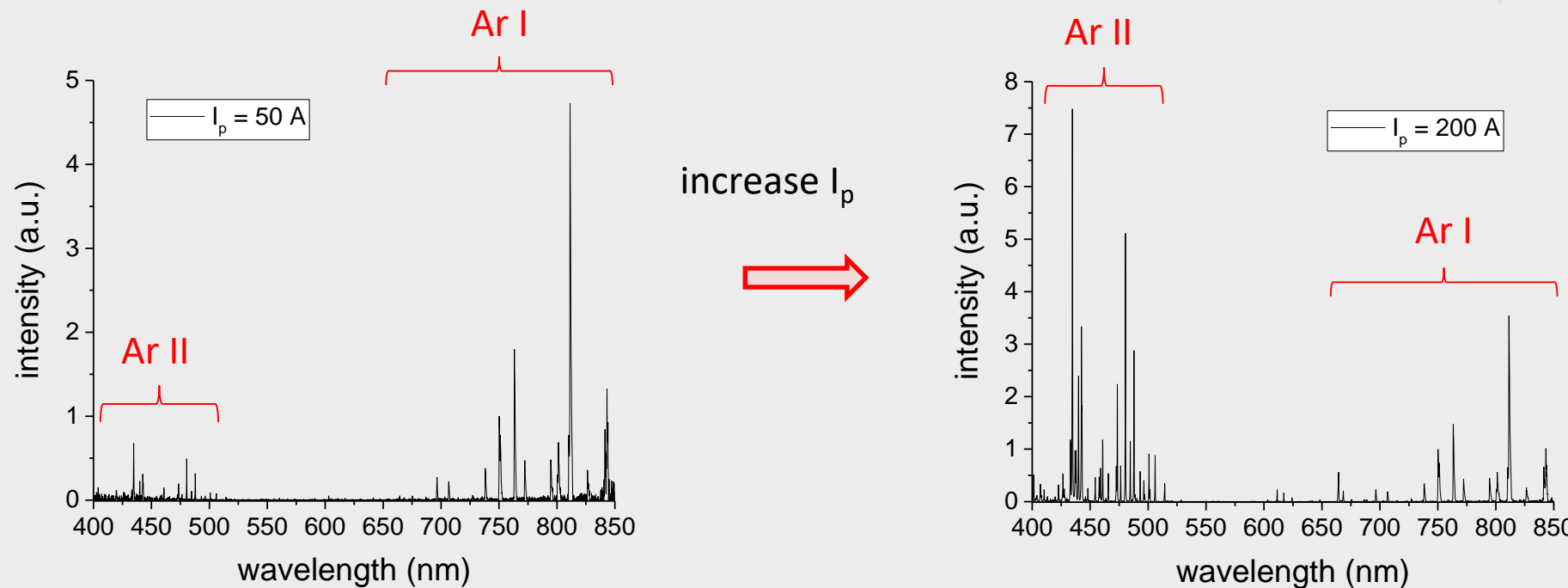
# H molecular energy levels



K. Sawada and M. Goto, Atoms 4 29 (2016)

# CR modeling including Ar and Ar<sup>+</sup> : Next works

Measured spectra in KAERI PBIF



As plasma current  $I_p$  increases, intensities of Ar ion lines dominate over those of Ar neutral lines

**Significant change between spectra intensities of Ar I and Ar II lines** are shown depending on the gas flow rate and electron density **around 487 nm** wavelengths from a plasma device in **Prof. G. Yun's team**.

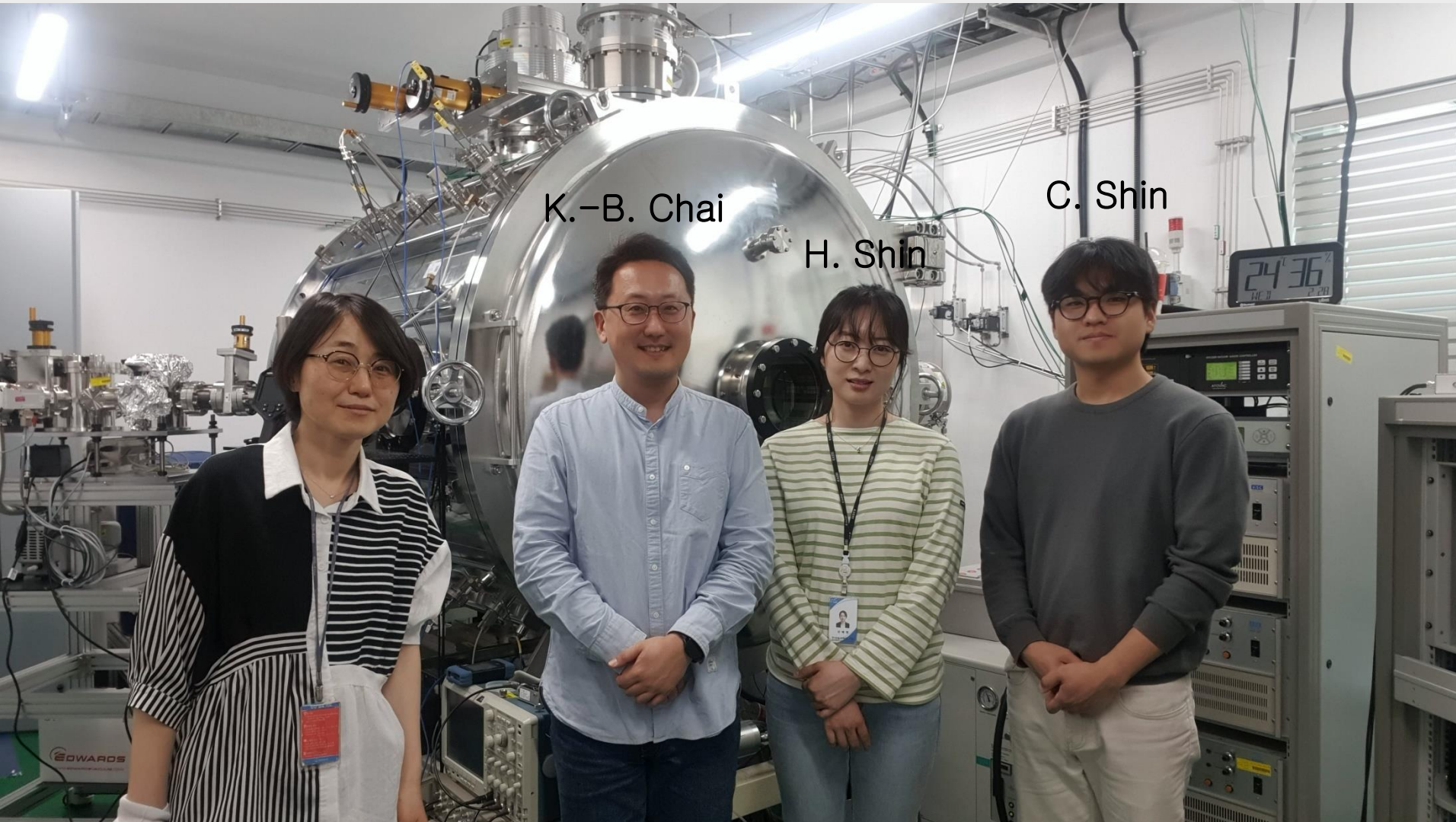
→ need to **extend our CR model to include both Ar and Ar ions** for the analysis of the spectral behavior by **collaboration with Prof. Yun's team**



## Summary and outlook

- CR modeling for highly charged ions from EBIT and atomic data are instructed for some selected examples. Detailed close collaboration of us with EBIT team will be desirable.
- Our developed CR model for low temperature, low density Ar, He, H/D plasma are described, which solves nonlinear steady-state balance equations including radiation trapping and heavy particle collisional ionization.
- The CR modeling for Ar will be extended to those for the both Ar and Ar<sup>+</sup> in highly excited states by the collaboration with Prof. G. Yun's team.

# Our group members



Theoretical calculation

Experimental measurements and analysis